












## RESEARCH ARTICLE

WILEY

# Evaluating input data sources for isotope-enabled rainfall-runoff models

Andrew Watson<sup>1</sup>  | Christian Birkel<sup>2,3</sup>  | Saul Arciniega-Esparza<sup>4</sup>  |  
Jan de Waal<sup>5</sup>  | Jodie Miller<sup>6</sup>  | Yuliya Vystavna<sup>6</sup>  | Jared van Rooyen<sup>7</sup>  |  
Angela Welham<sup>8</sup>  | Hayoung Bong<sup>9,10</sup>  | Kei Yoshimura<sup>9</sup>  |  
Jörg Helmschrot<sup>1,11</sup>  | Annika Künne<sup>12</sup>  | Sven Kralisch<sup>13</sup> 

<sup>1</sup>School for Climate Studies, Stellenbosch University, Matieland, South Africa<sup>2</sup>Department of Geography, University of Costa Rica, San Jose, Costa Rica<sup>3</sup>Department of Ecohydrology and Biogeochemistry, Institute for Freshwater Ecology and Inland Fisheries (IGB), Berlin, Germany<sup>4</sup>Hydrogeology Group, Faculty of Engineering, National Autonomous University of Mexico, Mexico City, Mexico<sup>5</sup>Department of Geography and Environmental Studies, Stellenbosch University, Stellenbosch, South Africa<sup>6</sup>Isotope Hydrology Section, International Atomic Energy Agency, Isotope Hydrology Section, Vienna International Centre, Vienna, Austria<sup>7</sup>Department of Water Resources and Drinking Water, Swiss Federal Institute of Aquatic Science and Technology (Eawag), Dübendorf, Switzerland<sup>8</sup>Department of Earth Sciences, Stellenbosch University, Stellenbosch, Western Cape, South Africa<sup>9</sup>Institute of Industrial Science, The University of Tokyo, Tokyo, Japan<sup>10</sup>Goddard Institute for Space Studies, NASA, NASA Goddard Institute for Space Studies, New York, New York, USA<sup>11</sup>Institute of Meteorology and Climate Research, Karlsruhe Institute of Technology, Karlsruhe, Germany<sup>12</sup>Institute of Geography, Friedrich-Schiller University Jena, Jena, Germany<sup>13</sup>Flood Prediction Centre, State Office for Environment, Mining and Nature Conservation, Jena, Germany**Correspondence**

Andrew Watson, School for Climate Studies,  
Stellenbosch University, Matieland 7602,  
South Africa.

Email: [awatson@sun.ac.za](mailto:awatson@sun.ac.za)

**Funding information**

European Union, Grant/Award Number: GA  
101082048; UNESCO, Grant/Award Number:  
4500461954; Water Research Commission,  
Grant/Award Number: C2024/205-01587;  
International Atomic Energy Agency,  
Grant/Award Number: CRP 31004

**Abstract**

Isotope-enabled models provide a means to generate robust hydrological simulations. However, daily isotope-enabled rainfall-runoff models applied to larger spatial scales (>100 km<sup>2</sup>) require more input data than conventional non-isotope models in the form of precipitation isotope time series, which are difficult to generate even with point station measurements. Spatially distributed isotope data can be circumvented by isotope-enabled climate models. Here, we evaluate the hydrological simulations of the J2000-isotope enabled hydrological model driven with data from corrected and un-corrected isotope-enabled global and regional climate models (isotope-enabled global spectral model [IsoGSM] and isotope-enabled regional spectral model [IsoRSM], respectively) compared with 1 year of measured reference station and a yearly average precipitation isotope input for a pilot site, the data-scarce sub-humid Eerste River catchment in South Africa. The models driven by all input products performed well for upstream and downstream discharge gauges with Nash Sutcliffe efficiency (NSE) from 0.58 to 0.85 and LogNSE of 0.66 to 0.93. The simulated  $\delta^2\text{H}$

This is an open access article under the terms of the [Creative Commons Attribution](https://creativecommons.org/licenses/by/4.0/) License, which permits use, distribution and reproduction in any medium, provided the original work is properly cited.

© 2024 The Author(s). *Hydrological Processes* published by John Wiley & Sons Ltd.

stream isotopes using the reference J2000-iso and J2000-isoRSM were good for the main river with a stream Kling Gupta efficiency (KGE) of between 0.4–0.9 and the top 100 Monte Carlo simulations varying by around 5‰ for  $\delta^2\text{H}$ . For smaller tributaries the model was unable to capture the measured stream isotopes due to biased precipitation isotope inputs. Adjusting the J2000-iso with a bias corrected IsoRSM improved the stream and groundwater isotope simulation and outperformed the model driven by an average yearly precipitation isotope input. Differences in simulated hydrological processes were only evident between the models when evaluating percolation with unrealistic simulations for the standard J2000 model. While the regional climate model is computationally more intensive than its global counterpart, it provided better stream isotope simulations and improvements to simulated percolation. Our results indicate that isotope-enabled climate models can provide useful input data in data scarce regions for hydrological models, where improved water management to address climate change impacts is needed.

#### KEYWORDS

isotope tracers, isotope-enabled modelling, Mediterranean southern Africa, model uncertainty, rainfall-runoff modelling

## 1 | INTRODUCTION

Stable isotopes, being natural constituents of water, act as sensitive tracers of the hydrological cycle due to their responsiveness to temperature, where the fractionation of heavy to light isotopes is influenced by condensation and evaporation (Dansgaard, 1964; Jasechko et al., 2013). The integration of stable isotopes into hydrological models therefore has the potential to improve the simulation of the hydrological cycle by considering the impact of evaporation and source mixing on moisture feedback between the atmosphere and hydrosphere (Kuppel et al., 2018; Nan et al., 2021b; Stadnyk et al., 2013; Watson, Kralisch, et al., 2024). While isotope-enabled models are beneficial in producing more robust simulations of hydrological processes and water balance estimates (Birkel & Soulsby, 2015; Watson et al., 2023), their more widespread application and use at larger catchment scales beyond 100 km<sup>2</sup> is limited by the availability of spatially-distributed precipitation isotope data (Yang et al., 2023).

The global network of precipitation isotope data (GNIP), managed by the International Atomic Energy Agency, is a global database of stable isotope precipitation data at a monthly resolution (International Atomic Energy Agency, 2008; Vystavna et al., 2020) and some more recent daily datasets. The database is reasonably extensive, covering 100 countries with over 900 monitoring stations across tropical, temperate, arid and polar regions. As such it represents an invaluable data source for monthly water balance-type assessments. However, for hydrodynamic modelling, there is the need for catchment specific precipitation isotope data at daily or sub-daily time resolution (Yang et al., 2023). Furthermore, such higher-resolution precipitation isotope

data is also needed to effectively correct and apply isotope-enabled climate models for use with isotope-enabled hydrological models (Arciniega-esparza et al., 2023; Delavau et al., 2017). Extensive supplementary isotope sampling campaigns and continuous monitoring programs in countries such as Canada, Scotland and Germany have supported the long-term use of daily isotope-enabled models (Birkel et al., 2018; Holmes et al., 2023; Koeniger et al., 2022). However, in most developing countries such as South Africa, Costa Rica and Mexico, the limited availability of daily isotope precipitation data has restricted the development and application of isotope-enabled rainfall-runoff models.

As a primary source of isotopes for precipitation, an isotope-enabled global spectral model (IsoGSM: Yoshimura & Kanamitsu, 2008) can provide globally-distributed, sub-daily scale precipitation isotope estimates (50 km grid scale) for catchments with spatially insufficient observation data. Like its non-isotope enabled climate model counterparts, the isotope-enabled regional spectral model, IsoRSM (Yoshimura et al., 2010) is a regional version of the global IsoGSM applied to a smaller domain at a higher spatial resolution (10 km). The regional model is computationally more intensive and requires setting initial and boundary conditions in the generation of high-resolution precipitation isotope estimates. IsoRSM can therefore reduce downscaling errors for sub-grid estimation of isotope precipitation at local scales by considering complex topography and low-pressure systems (Bong et al., 2024). Nonetheless, IsoGSM and IsoRSM require testing for their use in isotope-enabled rainfall-runoff models and whether they, despite the spatial and temporal mismatch between the input data source and hydrological model scale, improve overall model robustness. Similar to non-isotope climate model

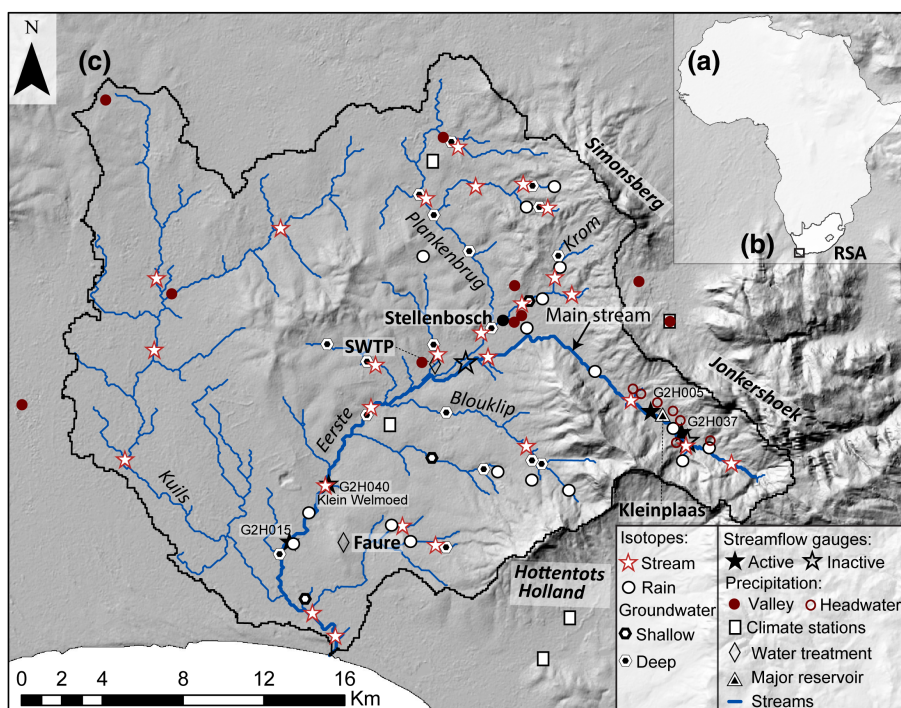
correction with for example, quantile mapping (Gudmundsson et al., 2012), the IsoGSM and IsoRSM model outputs may need to be corrected for biases before use in hydrological models (e.g., Delavau et al., 2017). Such corrections are needed to capture local climate conditions. However, it is necessary to identify and test best practices to adjust regional and global isotope enabled-climate models to better reflect local climates but also consider whether the addition of precipitation isotopes improves hydrological models.

In this study, we assess the potential use of IsoRSM and IsoGSM as inputs for isotope-enabled rainfall-runoff modelling. The evaluation was done in the Mediterranean Eerste River catchment in the Western Cape of South Africa. The simulation of percolation/groundwater recharge is of particular interest in the Western Cape due to the numerous pressures on groundwater resources including population growth, agricultural expansion and climate change (Miller et al., 2018; Watson et al., 2018, 2022). The combined pressures of these three factors contributes to the increased urgency to generate robust early warning forecasting systems linked to climate projections. The Eerste catchment has high-quality climate data but does not have the available extended precipitation isotope time series necessary to run an isotope-enabled hydrological model. Therefore, the hydrological simulations of the J2000-iso and stream water isotope fit using IsoGSM and IsoRSM simulated precipitation isotope data, were benchmarked against 2023 time series of measured precipitation isotope data, which is the only measured time series available. A yearly average precipitation isotope value from IsoRSM was used to evaluate the model parameter's ability to dampen or amplify the simulated stream isotope composition, according to the measure data and the added benefit of including the simulation of stable water isotopes.

## 2 | ENVIRONMENTAL SETTING

The Eerste River covers the southern part of the Berg River Water Management Area (WMA), falling within the Western Cape province of South Africa (Figure 1a,b), where Stellenbosch is the dominant urban settlement (population: 155 000) in the catchment (Figure 1c). The Eerste catchment area is 620 km<sup>2</sup>, draining the mountain ranges of the Jonkershoek (1589 m.a.s.l.) in the east, Simonsberg (1399 m.a.s.l.) in the north and Hottentot-Holland (1590 m.a.s.l.) in the south. Anthropogenic features which impact and modify the natural flow of the Eerste River include: the Kleinplaas (0.37 Mm<sup>3</sup>) reservoir, as well as the Stellenbosch wastewater plant (SWTP: capacity 35 ML/day), Faure (capacity 500 ML/day) treatment works, and a small channel used for residential irrigation (leiwater) in Stellenbosch (Figure 1c). Geological features in the catchment include the Cambrian Table Mountain Group sandstones (TMG) which dominate the mountain ranges, while the Tygerberg formation is dominant in the valley and is comprised mainly of shales, fine grade greywacke and quartzite (Johnson & Thamm, 2006). The Cape Granite Suite has intruded the Tygerberg formation and outcrops in low-lying places. Towards the coast, the Cape Flats aquifer is present which is a highly productive alluvial aquifer, used mainly for irrigation and is underlain by the Tygerberg and Cape Granite suite. Mean annual precipitation (MAP) varies between 2000 to 3000 mm/year in the Jonkershoek headwaters, around 650–900 mm/year in Stellenbosch, while in the western portion of the catchment precipitation is between 500 and 650 mm/year (Figure 2a) (Lynch, 2004). Across the entire catchment precipitation is around 774 mm/year, where 2023 had the second highest amount of precipitation for the last 29 years (1995–2023) with 1034 mm. The Eerste falls within the winter rainfall section of the

**FIGURE 1** Location of the Western Cape within (a) Africa and (b) South Africa, (c) the Eerste River catchment including the town of Stellenbosch, water treatment works (Faure) and Stellenbosch water treatment plant (SWTP) main river stem of the Eerste River, the Eerste's tributaries, streamflow gauging stations, available climate and precipitation stations, the collected stable isotopes of rain water, stream water and groundwater (shallow and deep), Kleinplaas Dam and mountain ranges of Simonsberg, Jonkershoek and Hottentots Holland.



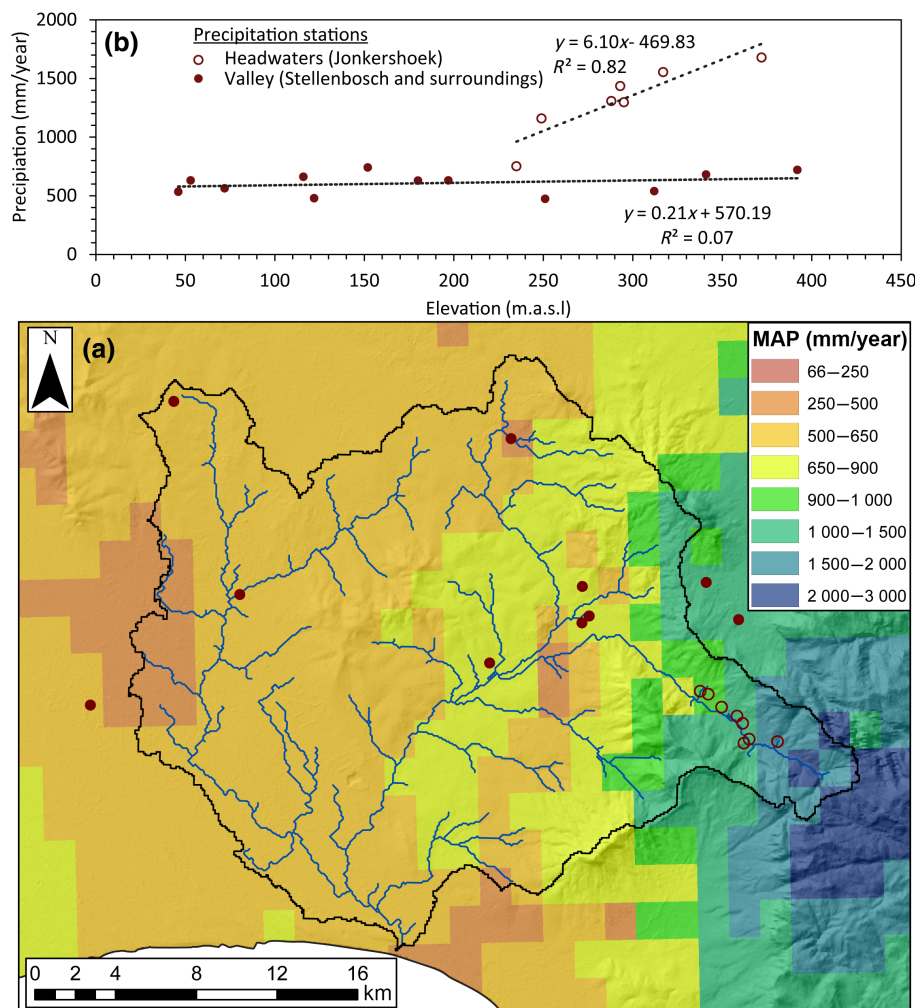


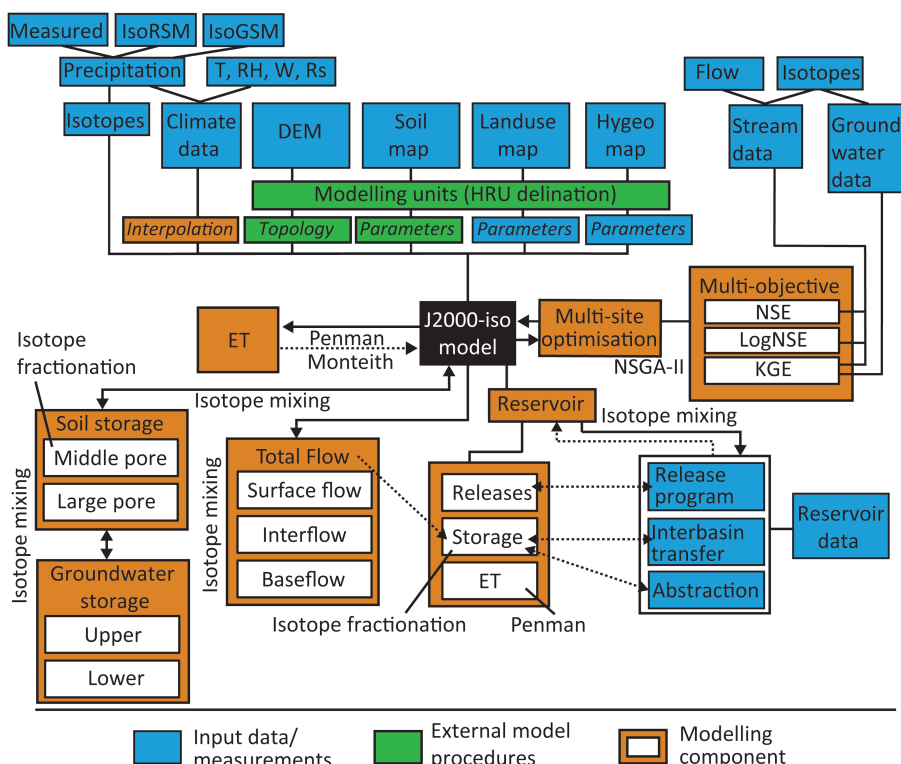
**FIGURE 2** (a) Mean annual precipitation (Lynch, 2004) for the Eerste River including the locations of headwater and valley precipitation stations and (b) a regression of the annual precipitation and the station's elevation showing altitude effects for the headwater stations.

Western Cape (Roffe et al., 2019), having a Mediterranean climate where 50% of MAP is received in the months June, July and August. Precipitation stations in the headwaters of the catchment exhibit a linear relationship ( $R = 0.83$ ) between altitude and MAP, while in the valley altitude and MAP have limited correlation ( $R = 0.07$ ) (Figure 2b). Groundwater recharge rates are between 13% and 27% of MAP for the TMG in the region (Miller et al., 2017; Watson et al., 2019; Weaver & Talma, 2005; Wu & Xu, 2005), compared with the alluvial aquifer which is between 2% and 5.6% of MAP (Conrad et al., 2004; Watson et al., 2020). While limited information is available on groundwater recharge for the Tygerberg formation, estimates of between 6% and 8% of MAP have been made for the Malmesbury formation which is a similar shale aquifer found in the northern parts of the Western Cape (Conrad et al., 2019). Groundwater recharge for the Cape Granite suite is largely regarded as low, due to most boreholes (42%) yielding <2 L/s (Department of Water and Sanitation [DWS] groundwater dictionary). The most prevalent land use in the catchment is cultivated vines as much of the catchment has been converted into agriculture (33%). For additional information on climate and similarities between Eerste and other surrounding catchments refer to Watson et al. (2021).

### 3 | MATERIALS AND METHODS

The study uses J2000-iso (Watson et al., 2023; Watson, Kralisch, et al., 2024), an isotope-enabled version of the JAMS/J2000 rainfall-runoff model (Kralisch & Krause, 2006; Krause & Kralisch, 2005), to simulate streamflow and streamflow isotopes within the Eerste River. The JAMS/J2000 is a modular object-oriented conceptual rainfall-runoff model which can be used to simulate hydrological and hillslope processes on a catchment scale Figure S1. The model uses hydrological response units (HRUs) as entities of homogeneous topology, hydrogeology, soil and land use characteristics. HRUs are paired with a topological routing scheme in the model to simulate catchment flow dynamics (Pfennig et al., 2009). To account for the impact of the upstream reservoir (Kleinplaas Dam) within the Eerste, new components were developed to simulate water storage, change in cross-sectional area, evaporation, inter-basin transfer, reservoir inflow and outflow from the reach (Figure 3). The isotope-enabled version differs from the standard conceptual rainfall-runoff model as it includes the simulation of stable isotope fluxes ( $\delta^2\text{H}$ ) using a mixing cell approach. Further, isotope fractionation within the soil and for open-water bodies (reservoir) horizons is considered using a combination of the

**FIGURE 3** An overview of the modelling approach including the input data for the J2000-iso, the inclusion of isotope fractionation during water evaporation simulation (from the soil and reservoir), isotope mixing within soil pore storages, groundwater storage and total flows from surface runoff, interflow and baseflow, the addition of reservoir operations (release program, inter-basin transfer and abstraction), the multi-site (three stream gauges) multi-objective calibration (Nash Sutcliffe efficiency (NSE) in standard form; Nash, 1970, logarithmic form: LogNSE and the Kling Gupta efficiency: KGE, Gupta et al., 2009) using stream discharge data and stream isotope data as well as groundwater isotope data used for validation. DEM, Digital Elevation Model; ET, evapotranspiration; IsoGSM, isotope-enabled global spectral model; IsoRSM, isotope-enabled regional spectral model; KGE, Kling Gupta efficiency; NSE, Nash Sutcliffe Efficiency in standard form; NSGA, non-dominated sorting genetic algorithm.



Craig–Gordon model (1965) to account for the impact of evaporation on isotope composition. Additionally, the isotope-enabled version considers the mixing of isotopes within the components and storages of the model, following the same defined topological routing scheme developed in the HRU delineation. For further details on the isotope enabled version of the model refer to Watson, Kralisch, et al. (2024) as a brief overview is provided in Section 3.3. Details on the HRU delineation and climate regionalization are available in Watson et al. (2020).

### 3.1 | Model setup

#### 3.1.1 | Climate

Mean daily temperature, relative humidity and windspeed, maximum and minimum temperature as well as total solar radiation and precipitation for the periods 01 January 2011 to 31 December 2023 were collected from local weather bureaus, research institutes and private companies operating weather stations in the catchment (Table 1). The availability of data from the stations was not continuous and several stations did not have records for the entire analysis period. Between the period 1997 to 2011 records in the Jonkershoek, the headwaters of the catchment, were not available and the nearest station to the headwater sub-basin was in Stellenbosch. But on average the precipitation station to HRU distance was 10–12.5 km, while the mean temperature was 17 to 22 km across the catchment suggesting a good station coverage based on HRU to station distance recommendations from Watson et al (2020) for the Western Cape.

#### 3.1.2 | Streamflow

Streamflow data were available from six streamflow gauging stations within the catchment (Figure 1c). Headwater stations include G2H008 and G2H037 maintained by the South African DWS. Downstream stations include G2H005, G2H020, G2H040 and G2H015. Records from Jonkershoek G2H037 and Kleinwelmoed G2H040 were used for the calibration and validation (due to the availability of data after 1997), whilst records from Kleinplaas G2H005 were used to validate the simulated reservoir outflow rate.

#### 3.1.3 | Isotope data and sampling

Stable water isotope ( $\delta^{18}\text{O}$  and  $\delta^2\text{H}$ ) samples were collected from five sample campaigns during the dry and wet seasons of March, June, September and November 2023. Overall, a total of 264 cumulative daily rainfall (i.e., total rainfall over 24 h from 08:00 SAST), 57 surface water, 52 deep groundwater and 5 shallow groundwater samples were collected. These include spatial isotope monitoring with 17 precipitation, 29 surface water, 21 deep groundwater and three shallow groundwater samples. Of these samples more than two were collected at 20 surface water and 17 deep groundwater sites, with no shallow groundwater site sampled more than twice during 2023. Farmers and locals collected the rainwater samples from 19 January 2023 to 29 October 2023. Groundwater samples are assumed to represent a single aquifer unit as the screen depths were unknown (Miller et al., 2022). A 50 mL clean syringe with a 0.45  $\mu\text{m}$  cellulose acetate (CA) filter was used to filter the water samples into a clean

**TABLE 1** The input data for the J2000-iso model including stationary and non-stationary data as well as a description of the data source and reference.

	Dataset	Description	Stationary/non-stationary	Reference
1	DEM-SRTM 90 m	Digital Elevation Model	Stationary	N/A
2	Land use	South Africa National Land-Cover dataset 2013–2014	Stationary	GeoTerraImage, 2015
3	Geology/ Hydrogeology	Council for Geosciences 1: 250 000 map	Stationary	Theron, 1990
4	Soil	Harmonized World Soil Database	Stationary	(Batjes et al., 2012)
5	Climate	South Africa Weather Services, National Oceanic Atmospheric Administration, South African Environmental Observation Network, Hortec	Non-stationary	N/A
6	Streamflow	Department of Water Affairs and Sanitation (DWS)	Non-stationary	N/A
7	Dam operations	Stellenbosch Municipality, DWS	Non-stationary	N/A
8	Precipitation isotopes	IsoRSM/IsoGSM	Non-stationary	(Yoshimura & Kanamitsu, 2008)
9	Isotope samples	Precipitation, Stream water, groundwater, reservoir water—Stellenbosch University	Non-stationary	N/A

15 mL polypropylene (PP) falcon tube, followed by storage <4°C until analysis. The Los Gatos Research Triple Liquid Water Isotope Analyser (LGR T-LWIA-24D) and cavity ring-down spectroscopy (CRDS) (at Biogeochemistry Research Infrastructure Platform [BIOGRIP] Soil and Water Node at Stellenbosch University Central Analytical Facility) were used to measure  $\delta^{18}\text{O}$  and  $\delta^2\text{H}$  in precipitation, groundwater and stream water.

### 3.1.4 | Hydrogeology

The groundwater component of the J2K uses of two conceptual storages, where RG1 represents fast moving groundwater from the upper primary aquifer and RG2 represents slow moving groundwater from a lower basement aquifer. The input hydrogeological data for the model included the maximum storage capacity of the upper and lower aquifer (RG1max and RG2max), and the storage coefficients of RG1\_k and RG2\_k, where spatial extents were determined using a locally obtained geological map (Table 1). Regional literature and previous J2000 models were used to determine RG1max, RG2max and initial values of RG1\_k and RG2\_k (Conrad et al., 2004; SRK, 2009; Watson et al., 2018, 2020). A scaling factor for each aquifer unit was introduced to calibrate the storage coefficient of RG1 and RG2 (Table 2). As an additional means to validate groundwater simulation we used MTT indicator according to Herrmann and Stichler (1981).

### 3.1.5 | Soils

The harmonized world soil database (HSWD: Batjes et al., 2012) was used as the input soil dataset. Soil depth, texture (sand%, silt% and clay%) were used to determine the water holding capacity and air capacity as middle pore storage (MPS) and large pore storage (LPS) for

an A and B horizon. The Rosetta lite pedotransfer function (Schaap et al., 2001) within Hydrus-1D (Simunek et al., 2011) was used to estimate these storages using a soil-water retention curve (theta vs. depth) and emptied via a constant upper and lower head boundary condition for each soil type. MPS was determined by subtracting the water holding capacity at 15 000 and 60 mbar from the soil-water retention curve. LPS was determined by subtracting water holding capacity at 0 and 60 mbar from the same soil water retention curve. These capacities were then multiplied by the effective soil depth reported in the HSWD. A calibration factor (AC\_Adaptation and FC\_Adaptation) was used to scale the effective water holding capacity of the soil storages (collectively) in the absence of detailed soil physical data (Table 2).

### 3.1.6 | Land use

The different land use classes within the catchment were attained from the South African National Land-Cover dataset for 2013 to 2014 (GeoTerraImage, 2015). The model requires land use parameters to determine interception and calculate potential evapotranspiration (ET). The interception module uses leaf area index (LAI) for different vegetational growing periods (1–4; Julian days 110, 150, 250 and 280 for regions <400 m.a.s.l.). The calculation of potential ET requires land use: (1) albedo (%), (2) monthly surface resistances assuming sufficient water supply, (3) effective height for growth periods, (4) root depth and (5) sealed grade value (% impervious areas). These different parameters per land use class were estimated using local and global literature (Amer & Hatfield, 2004; Johnson, 1983; Munitz et al., 2017; Van Zyl, 1984). To account for the vegetation's ability to reduce transpiration during soil-water stress, a calibration factor (soilLinRed) was used to linearly reduce potential ET based on the relative soil moisture of MPS (Table 2).

**TABLE 2** Summary of the model parameters used for the J2000-isoCal, J2000-isoVal, J2000-isoRSM, J2000-isoGSM, J2000-isoRSM BiasC and RSM\_Null case as well as the optimal parameters attained from the non-dominated sorting genetic algorithm-II (NSGA-II): (Deb et al., 2002) and lower and upper bounds used for the Monte Carlo analysis (MCA).

Name of parameter	Type	Description of parameter	J2000-iso Calibration range	Cal Optimal value	MCA parameter sets			Val Optimal value	RSM Optimal value	GSM Optimal value	RSM BiasC Optimal value	RSM_Null case Optimal value
					MCA lower bounds	MCA upper bounds						
AC_Adaptation	Soil-water	multiplies the volume of the large pore storage of soil	0.7-1.5 3*	2.97	2.67	3.27	2.96	2.98	2.99	2.87	2.87	1.59
FC_Adaptation	Soil-water	multiplies the volume of the middle pore storage of soil	0.7-1.5 3*	2.90	2.61	3.19	0.85	2.64	2.32	2.57	2.57	2.87
soilInRed	ET	Actual ET parameter, governing the reduction of potential ET according to the soil moisture	0-1	0.12	0.11	0.13	0.03	0.20	0.24	0.02	0.02	0.40
soilDiffMPSLPS	Soil-water	MPS/LPS diffusion coefficient	0-10	1.39	1.25	1.53	0.07	6.49	9.98	6.49	6.49	6.49
soilDistMPSLPS	Soil-water	MPS/LPS distribution coefficient for inflow	0-10	0.51	0.46	0.56	3.60	4.59	8.20E-05	4.59	4.59	4.59
soilMaxInfSummer	Soil-water	The maximum infiltration capacity of soil in the summer period (northern hemisphere)	0-200	127.93	115.14		161.69	132.77	197.84	132.77	132.77	132.77
soilMaxInfWinter	Soil-water	The maximum infiltration capacity of soil in the winter period (northern hemisphere)	0-200	193.62	174.26		100.12	88.80	172.66	88.80	88.80	88.80
soilConcRD1	Soil-water	Surface runoff delay parameter	0.5-2	1.98	1.78	2.17	1.99	1.28	1.98	1.37	1.37	
soilConcRD2	Soil-water	Interflow delay parameter	0.5-5	3.94	3.54	4.33	4.24	3.80	3.78	2.90	2.90	
soilOutLPS	Soil-water	Outflow parameter of the large pore storage	0-10	0.75	0.67	0.82	1.72	3.53	1.00	3.53	3.53	3.53
soilMaxPerc	Soil-water	Conductivity adaption parameter for leaching water to the groundwater storage	0-20	19.28	17.36	21.21	14.83	19.98	17.10	18.77	18.77	17.41
soilLatVert	Soil-water	Distribution coefficient for LPS outflow to lateral and vertical flow path	0.1-10	1.39	1.25	1.53	1.53	0.96	1.60	0.66	0.66	2.10
gwRG1RG2dist	Groundwater	distribution parameter for the slow and fast groundwater runoff	0-1	0.96	0.87	1.06	0.96	0.95	0.98	0.95	0.95	0.95
gwRG1Fact	Groundwater	fast groundwater (slow interflow) delay	0-10	7.97	7.17	8.76	0.55	6.08	5.46	6.08	6.08	6.08
gwRG2Fact	Groundwater	Base flow delay	0-10	8.42	7.58	9.26	3.03	3.52	7.89	3.52	3.52	3.52
flowrouteTA	Flow routing	Stream routing parameter (overall dampening of the hydrograph)	0-20	16.24	14.61	17.86	12.93	14.80	19.78	6.66	6.66	
RG1_k	Groundwater	Outflow of fast groundwater	0.1-3	0.97	0.88	1.07	0.99	0.98	2.96	0.20	0.20	0.98
RG2_k	Groundwater	Outflow of slow groundwater	0.1-3	0.99	0.90	1.09	1.00	0.99	0.99	0.99	0.99	1.00
RG1RG2_max	Groundwater	Storage capacity of the upper and lower groundwater store	0.1-5*	4.58	4.12	5.04	2.37	1.18	3.43	4.04	4.04	4.38
isoMixHruReach	Isotope	Mixing between hrus and reaches	0.1-1	0.58	0.52	0.64	0.66	0.14	0.86	0.42	0.42	0.71
isoMixProp	Isotope	Mixing proportion for the isotope mixer	0.1-1	0.18	0.16	0.19	0.34	0.58	0.66	0.10	0.10	0.11

Note: \* and bold parameters not sensitive and not optimized in J2000-isoRSM BiasC and IsoRSM Null case. Abbreviations: ET, evapotranspiration; IsoGSM, isotope-enabled global spectral model; IsoRSM, isotope-enabled regional spectral model.

### 3.1.7 | Reanalysis nudging simulation for precipitation isotope data

Precipitation isotope data from IsoGSM spectrally nudged (Yoshimura & Kanamitsu, 2008) by ERA5 (Hersbach et al., 2020: 31 km resolution) and IsoRSM (10 km resolution) for the study catchment were provided by the University of Tokyo, high-resolution version of IsoGSM (Bong et al., 2024, horizontal spectral triangular truncation T248 equating to 0.47°, approximately 52.5 km at the Equator). IsoGSM data was clipped from an existing global library containing records from 01 January 1970 to 31 December 2023. Using IsoGSM output as a boundary condition, IsoRSM simulated an additional two model months prior to 2022 for spin-up, ensuring that by 01 January 2022, the model provided accurate and continuous results. This process completed a 2-year reconstruction from 01 January 2022 to 31 December 2023 for the catchment. The data from IsoGSM and IsoRSM were generated as separate NetCDF files, where the centroids of the pixels were extracted for input into J2000-iso. Two pixels from IsoGSM covered the entire study catchment, while the IsoRSM data included 16 pixels for the catchment. Whilst a range of different post-processing bias correction approaches were available (Gudmundsson et al., 2012) to correct both the isotope precipitation data as well as the amount of precipitation, quantile mapping was not used due to the temporal bias. Only the precipitation isotope data was sourced from IsoGSM and IsoRSM and not the precipitation amount due to the hit bias in low rainfall days and the potential issues in simulating streamflow (Figure 4a). To evaluate the benefits of providing external bias correction to the isotope data from IsoRSM, a linear correction of IsoRSM was applied and used in the J2000-isoRSM BiasC model (Figure 4b).

## 3.2 | Reservoir simulation

To consider the impact of the Kleinplaas Dam (Figure 1) on downstream flows and isotope compositions, a new reservoir component was developed. The reservoir component expands on the farm dam

component developed in Watson, Künne, et al. (2024) to include reservoir release, inter-basin transfer, domestic abstraction, mixing of isotopes and isotope fractionation while excluding abstractions for irrigation. The similarities between the farm dam and reservoir component includes the interpolation of surface area based on storage condition and the use of Penman (1948) for estimating surface water evaporation loss. The reservoir was simulated as a specific type of reach segment with additional properties, initial conditions and calculations. Within the reservoir reach the following data were added to the reach containing the Kleinplaas reservoir: (1) the capacity of the reservoir at full supply ( $R_{FS}$ ), (2) the maximum surface area of the reservoir ( $R_{s_{max}}$ ), (3) the minimum surface area of the reservoir at 10% capacity ( $R_{s_{min}}$ ), (4) the maximum release ( $R_{max\ out}$ ) from the reservoir taken from the DWS gauging records (G2H005), (5) the minimum release from the reservoir ( $R_{min\ out}$ ), (6) a monthly (12 values) average daily inter-basin transfer into the reservoir (data from DWS: G2H033) ( $R_{abs\ in}$ ) and (7) a monthly (12 values) average daily abstraction as municipal use ( $R_{abs\ out}$ ). The outflow from the dam ( $R_{out}$ ) was determined by interpolating across ( $R_{max\ out}$ ), ( $R_{min\ out}$ ),  $R_{FS}$  and actual storage condition ( $R_S$ ) as:

$$R_{out} = (R_{max\ out} - R_{min\ out}) \times \left( \frac{R_S}{R_{FS}} \right). \quad (1.1)$$

The reservoir was filled with water from the upstream reach, which was a calibrated reach, as well as inter-basin transfers. A variable, damTransferAdapt, limits inter-basin transfers to a fraction of the full capacity (0.85 used as a default). Additionally, damReleaseAdapt was used to stop dam releases during low storage conditions (0.1 used as a default).

## 3.3 | J2000-iso developments and components

The isotope components of the J2000-iso include: (1) a mixing component and (2) an isotope fractionation component. The isotope mixer integrates the isotope composition of water from various sources and

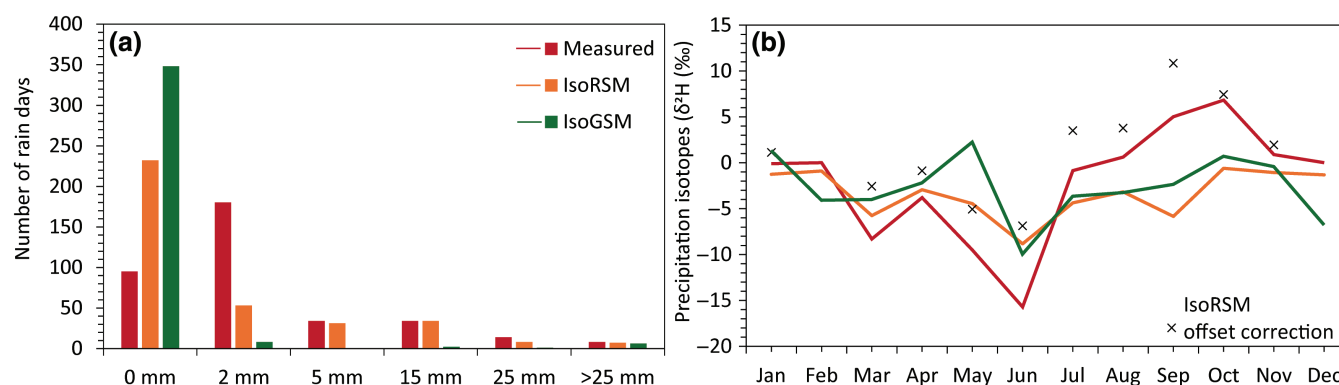


**FIGURE 4** (a) The number of days with zero rainfall, rainfall between 0 and 2, 2 and 5, 5 and 15, 15 and 25 and >25 mm for the measured precipitation, precipitation from IsoRSM and precipitation from IsoGSM for 2023 and (b) the monthly average measured precipitation isotope composition compared with compositions from IsoGSM and IsoRSM with the applied monthly correction factor. IsoGSM, isotope-enabled global spectral model; IsoRSM, isotope-enabled regional spectral model.

partitions within the model. The isotope mixer ensures that the isotope composition and water volume transport are maintained by water movement within a single HRU, between HRUs, from HRUs to reaches and within the model reaches themselves. The isotope mixer operates in one-direction for all components except soil water storage (MPS and LPS) as:

$$x = \frac{\text{Con}A_i \times \text{Vol}A_i + \text{Con}B_i \times \text{Vol}B_i}{\text{Vol}A_i + \text{Vol}B_i}, \quad (1.2)$$

where  $\text{Con}A_i$  is the isotope composition of component A,  $\text{Vol}A_i$  is the volume of component A,  $\text{Con}B_i$  is the isotope composition of component B,  $\text{Vol}B_i$  is the volume of component B. A mixing proportion, *isoMixProp*, calibrates the total water mixed affecting the translation of precipitation isotopes to depression storage (DPS), MPS, LPS and percolation. Additionally, an HRU to reach mixing proportion, *isoMixHruReach*, calibrates the total amount of water mixed by the HRUs with their corresponding reaches. Isotope fractionation was simulated from MPS storage using the liquid-vapour equilibrium and kinetic isotopic separation equation (Horita & Wesolowski, 1994) and after the Craig and Gordon (1965) model. For simulating isotope fractionation within the soil, the starting soil-water composition was derived from net rain and MPS, with an exchange factor (default 0.1). Fractionation from the reservoir considers an initial dam storage composition as the starting point with the initial value being defined as the overall simulated streamflow isotope composition at the first timestep. An initialisation (lead time) allows for the isotope compositions to stabilize before calibration with stream isotopes.

### 3.4 | Model calibration and validation

The model calibration utilized two gauging stations, where the upstream (Jonkershoek) and downstream (Kleinwelmoed) gauges were used for calibration. Additionally, 57 stream isotopes were included in the calibration. To compare the difference in the hydrological process simulation using different input data, five different calibrations were used in addition to a null case:

- i. J2000-isoCal with both streamflow and isotope calibration using measured precipitation isotopes,
- ii. J2000-isoVal with only streamflow calibration,
- iii. J2000-isoRSM with streamflow and isotope calibration using IsoRSM as precipitation isotope inputs,
- iv. J2000-isoGSM with both streamflow and isotope calibration using IsoGSM as precipitation isotope inputs,
- v. J2000-isoRSM biasC with both streamflow and isotope calibration using a linear bias corrected IsoRSM as well as calibration with only sensitive parameters (Table 2) and
  - a. A null case where the average yearly precipitation isotope composition from IsoRSM was used as the input into J2000-iso for calibration with only sensitive parameters.

The calibration made use of 10 000 model runs, utilizing the non-dominated sorting genetic algorithm II (NSGA-II: Deb et al., 2002) to collect Pareto-optimal solutions with the Nash Sutcliffe efficiency (NSE: Nash, 1970) and Log Nash Sutcliffe efficiency (LogNSE) used as model efficiency criteria to capture the peak and low flows of the measured streamflow. The Kling Gupta efficiency (KGE: Gupta et al., 2009) was used as model efficiency criteria to capture the general trends and variability between measured and simulated stream isotopes according to efficiency criteria from (IAEA, 2022). The model calibration was performed for 2023 utilizing the collected stable isotopes where 2022 was used as initialisation and warm-up using a duplication of the 2023 records. The gauging station records below the reservoir (outflow Kleinplaas) during 2023, as well as the 52 collected groundwater isotopes were used for validation. The selection of posterior samples from the pareto front included combining the average NSE, logNSE for each gauge and KGE from the stream isotopes and picking an optimal model run from the top 10 solutions including a validation from the reservoir outflow. Furthermore, a validation was performed from 2011 to 2021 using only the streamflow data. The calibration made use of a standard list of J2K parameters and literature parameter ranges (Table 2) (Watson et al., 2021), but included the tuning of the upper and lower groundwater outflow rate (RG1K and RG2K), as well as the maximum storage of the upper and lower groundwater store (RG1RG2\_max). Additionally, the isotope version of the model includes a parameter to mix a proportion of water from the HRUs to the reaches (*isoMixHruReach*) and a proportion factor used in mixing of isotopes between components and storages (*isoMixProp*) (Watson et al., 2024).

### 3.5 | Sensitivity analysis

A Monte Carlo analysis (MCA: Hornberger & Spear, 1981) was applied to the J2000-iso model to identify the sensitivity of each model parameter and variation in simulated stream isotopes for the best 100 MCA runs for a selected reach segment of importance. The optimal parameters from J2000-isoCal were used as the midpoint, where parameters were scaled randomly between the intervals [0.9, 1.1], with a maximum 10% increase or decrease in the selected optimal parameter sets. Like the calibration procedure, the sensitivity analysis used of NSE, LogNSE for the streamflow data and KGE for the stream isotopes as model efficiency criteria.

## 4 | RESULTS

### 4.1 | Stable water isotope characteristics of the Eerste catchment

In summer (March), surface waters in the study area exhibited  $\delta^{18}\text{O}$  ratios ranging from  $-5.24$  to  $-2.17\text{‰}$  and  $\delta^2\text{H}$  ratios from  $-20.93$  to  $-1.18\text{‰}$ , with an average d-excess of  $17.11\text{‰}$ , (Figure 5). Notably, the Plankenbrug and Krom Rivers, along with the downstream

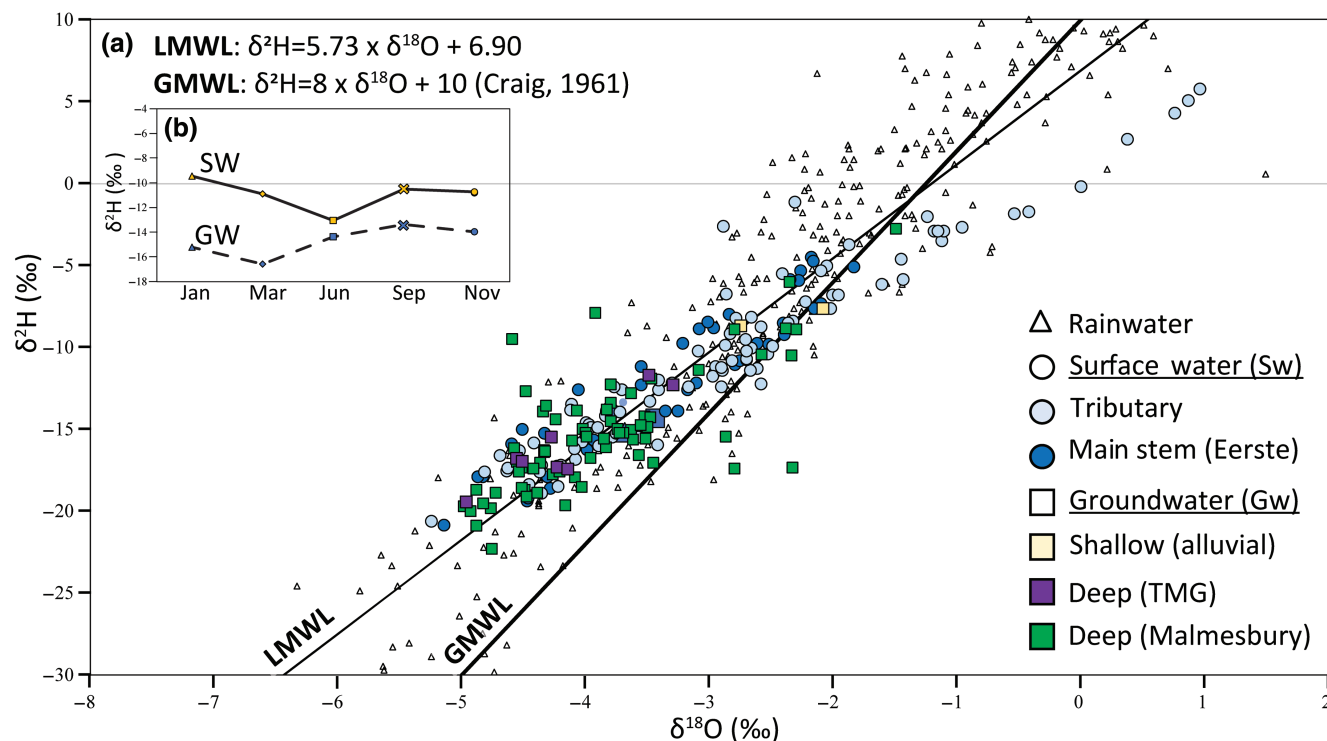


**FIGURE 5** (a) The collected stable isotopes of rainwater, surface water and groundwater split by samples collected along the main stem of the Eerste, samples collected on the Eerste's tributaries, groundwater samples collected from the shallow alluvial aquifer and deep samples for the Table Mountain Group and Malmesburg Group. (b) Box and whisker show the distribution of the sample isotope data for groundwater (GW) and surface water (SW) and (c) the temporal variability in the average surface water and groundwater samples. TMG, Table Mountain Group.

reaches, showed more enriched heavy isotope values ( $\delta^{18}\text{O} = -2.88$  to  $-2.23\text{‰}$  and  $\delta^2\text{H} = -8.27$  to  $-1.18\text{‰}$ ) in 2023, suggesting surface water evaporation with an average d-excess of 10.22‰. The upper Eerste River, influenced by the Jonkershoek Valley, supports the lower Eerste River, while Klienplaas Dam, with slightly different isotope values ( $\delta^{18}\text{O} = -2.17\text{‰}$ ;  $\delta^2\text{H} = -4.59\text{‰}$ ), mixes waters through the inter-basin transfers from Theewaterskloof (unknown isotope composition) with inflows from the catchment headwater ( $\delta^{18}\text{O} = -3.8\text{‰}$ ;  $\delta^2\text{H} = -14.8\text{‰}$ ). Groundwater  $\delta^{18}\text{O}$  values ranged from  $-4.98$  to  $1.49\text{‰}$  and  $\delta^2\text{H}$  values from  $-22.36$  to  $11.38\text{‰}$ , with the most (depleted) lowest heavy isotope values found in the upper and lower Eerste, Blaauwklippen and Veldwagters regions, indicating recharge from higher altitudes with a mean transit time of around 8 months.

## 4.2 | Simulated streamflow, stream and groundwater isotopes with different input sources

The five different models (J2000-isoCal, J2000-isoVal, J2000-isoRSM, J2000-isoGSM and J2000-isoRSM biasC) had good overall model stream NSEs for the upstream and downstream gauges (0.58–0.85) and moderate NSEs (0.4–0.45) at simulating reservoir outflows during calibration (Figure 6 and Table 3). Likewise, the different models had good LogNSE values (0.66–0.93) for the upstream and downstream

gauges but performed poorly at simulating reservoir outflows ( $-1.44$  to  $-0.6$ ) during calibration. Overall, streamflow KGE's were good across all gauges and models for the calibration period (0.23 to 0.88). Slight model performance reductions were evident across the validation for the five models, but overall NSE values were still good for the upstream and downstream gauges (0.57 to 0.75) with moderate NSE values (0.21 to 0.38) for the simulation of reservoir outflows (Figure 6 and Table 3). The LogNSE values for the first four models were likewise lower during the validation but were still good for the upstream and downstream gauges (0.47 to 0.77) but the models were still poor at simulating reservoir outflows ( $-1.81$  to  $-1.48$ ). J2000-isoRSM biasC performed the worst in terms of LogNSE with  $-0.23$  and  $0.16$  for the upstream and downstream gauges. Overall, the KGE values across all models and gauges were better during the validation as opposed to the calibration (0.41 to 0.86).

For J2000isoCal, simulated stream isotopes were, on average, between  $-8$  to  $-10\text{‰}$  for  $\delta^2\text{H}$  compared with  $-3.9$  to  $-2\text{‰}$  for  $\delta^2\text{H}$  in the headwaters (Figure 7a–e). The J2000-isoCal and J2000-isoRSM biasC models had the best isotope stream simulations with four to six points in the main channel having a good KGE (0.4–0.9), five to nine points with a moderate KGE (0.1 to 0.4) and seven to nine points along the tributaries with a poor KGE ( $<0.1$ ). While J2000-isoVal had a similar simulated stream isotope average to J2000-isoCal, it had one more point with a good KGE (six points), two points with a moderate KGE and 12 points with a poor KGE. J2000-isoRSM

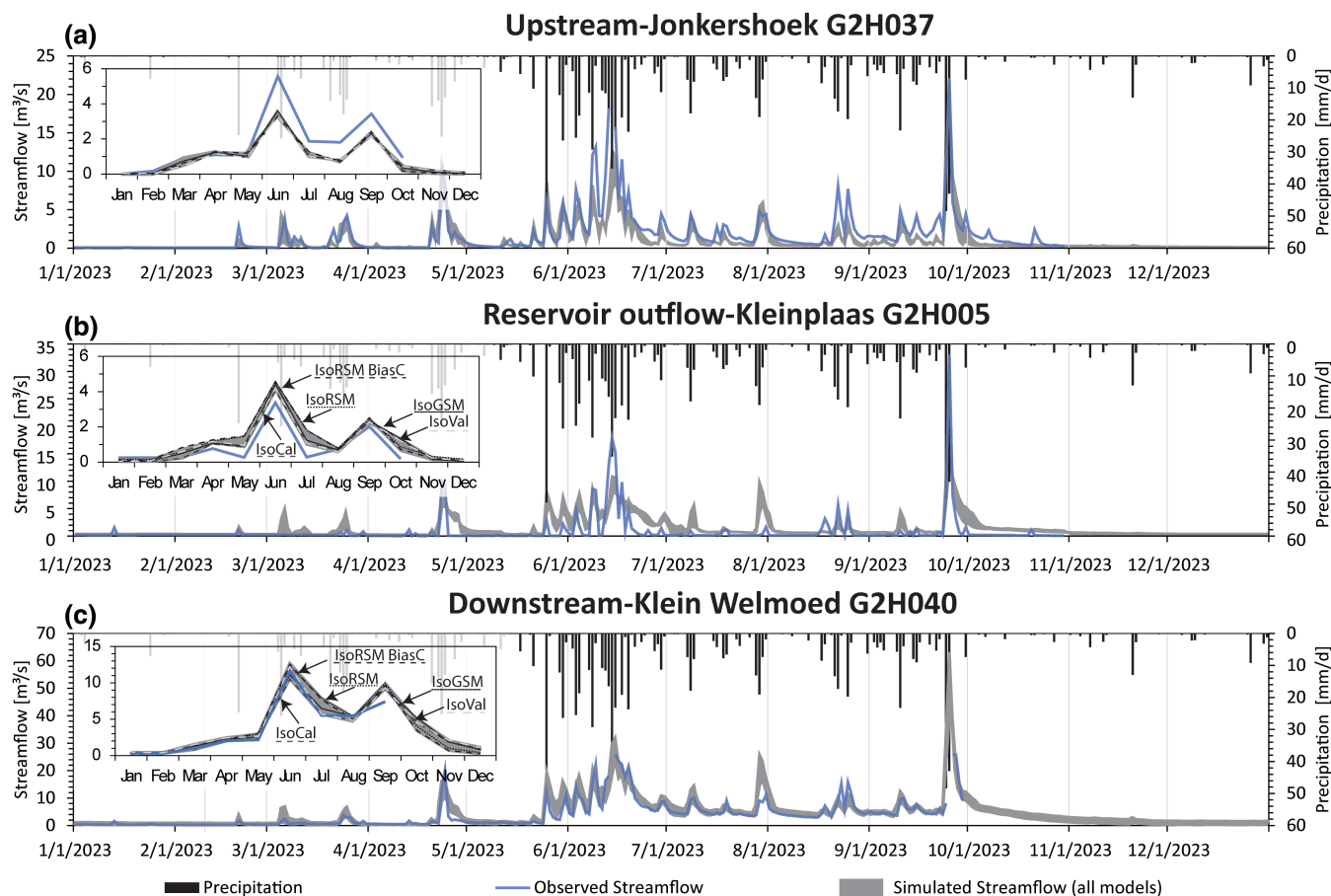


**FIGURE 6** The simulated daily and monthly streamflow using the J2000-isoCal (streamflow and isotope calibration), J2000-isoVal (streamflow calibration only), J2000-isoRSM (streamflow and isotope calibration using isotope data from IsoRSM), J2000-isoGSM (streamflow and isotope calibration using isotope data from IsoGSM), J2000-isoRSM biasC with both streamflow and isotope calibration using a linear bias corrected IsoRSM as well as calibration with only sensitive parameters, observed streamflow and measured precipitation for (a) upstream gauging station Jonkershoek (calibration point), (b) outflow from the Kleinplaas reservoir (validation only) and (c) the downstream gauging station Klein Welmoed for the year 2023 (initialisation 2022). IsoGSM, isotope-enabled global spectral model; IsoRSM, isotope-enabled regional spectral model.

performed like J2000-isoCal but with slightly more enriched light ( $^1\text{H}$ ) isotopes but fewer good KGE points. J2000-isoGSM was the worst at simulating stream isotopes with more depleted light ( $^1\text{H}$ ) isotopes, zero points with a good KGE and 19 with a poor KGE. The simulated stream isotope dynamics using J2000-isoCal show good agreement with measured isotopes during winter (01 June 2023) and less agreement during summer (01 March 2023) for reaches 744 and 876 (Figure 7ai-ei). J2000isoVal stream isotope dynamics show more enrichment of light ( $^1\text{H}$ ) but less seasonality than J2000-isoCal. Like J2000-isoVal, J2000-isoRSM shows more stream isotope variability and less seasonality. J2000-isoGSM stream isotopes dynamics had the highest variability for reach 876 (upstream) compared with 744 (downstream) and the worst agreement to stream isotope compositions. For the null case (average yearly precipitation isotope input), the J2000-iso model parameters influenced the simulated stream isotope composition as shown at reach 744 and 876 (Figure 7ei). But the overall performance driving J2000-iso with an average yearly precipitation input was poor across all the stream isotope collection points, with an average KGE of  $-0.07$ .

The deep groundwater isotopes were less well simulated by all the models with, on average, more depletion of light isotopes (Figure 8a-e). J2000-isoRSM, which had an average deep groundwater isotope value of  $-8.1\text{‰}$  for  $\delta^2\text{H}$ , had the best groundwater isotope simulation with six sites with above 0 KGE. J2000-isoRSM and J2000-isoRSM biasC performed like J2000-isoCal, which had an average deep groundwater isotope value of  $-6.2\text{‰}$  for  $\delta^2\text{H}$ . J2000-iso had an average deep groundwater isotope composition of  $-8.1\text{‰}$  for  $\delta^2\text{H}$  but performed worse than J2000-isoRSM in simulating groundwater isotope KGE. J2000-isoGSM showed the most depleted light isotopes and the worst temporal dynamics (Figure 8ai-ei).

#### 4.3 | Benchmarking simulated hydrological processes, percolation and parameter sensitivity using J2000-iso

The simulated ETET across the five models was, on average, between 622 and 674 mm/year, with the J2000-isoGSM and J2000-isoCal

**TABLE 3** Summary of the efficiency results (including the Nash Sutcliffe efficiency [NSE] in standard form; Nash, 1970, logarithmic form: LogNSE, the Kling Gupta efficiency [KGE], Gupta et al., 2009 and Bias) for the J2000-isoCal, J2000-isoVal, J2000-isoRSM, J2000-isoGSM, J2000-isoRSM BiasC and J2000-isoRSM Null case for the simulation at the upstream gauging station Jonkershoek, outflow from the Kleinplaas reservoir (validation only), the downstream gauging station Klein Welmoed, spatial isotopes for the stream, shallow groundwater (RG1: Validation only), deep groundwater (RG2: Validation only) used in the model evaluation for 2023 and 2011–2021.

Calibration (2023)																			
J2000-iso	Cal	Val			RSM			GSM			RSM_biasC			RSM_Null case					
	Gauges	Upstream	Dam*	Down stream	Upstream	Dam*	Down stream	Upstream	Dam*	Down stream	Upstream	Dam*	Down stream	Upstream	Dam*	Down stream			
Efficiency	NSE	0.58	0.45	0.83	0.60	0.42	0.85	0.68	0.55	0.68	0.60	0.40	0.82	0.68	0.50	0.74	0.62	0.38	0.84
	LogNSE	0.72	−0.87	0.93	0.81	−0.80	0.92	0.72	−0.60	0.90	0.82	−1.44	0.93	0.66	−0.62	0.87	0.77	−0.88	0.90
	Bias	−0.39	0.39	−0.03	−0.35	0.46	0.05	−0.37	0.69	0.11	−0.35	0.51	0.05	−0.36	0.70	0.11	−0.32	0.54	0.01
	KGE	0.41	0.40	0.88	0.45	0.35	0.91	0.56	0.25	0.80	0.46	0.32	0.86	0.55	0.23	0.82	0.49	0.30	0.92
	Isotopes	spatial points			spatial points			spatial points			spatial points			spatial points			spatial points		
	KGE	0.15	0.13			0.02			−0.30			0.23			−0.07				
	Bias	−0.50	−0.49			−0.53			−0.82			−0.46			−0.54				
	KGE	−0.23	−1.11			0.35			−0.03			0.33			0.51				
	RG1*																		
	KGE	−0.38	−0.64			−0.37			−0.15			−0.52			−0.26				
RG2*																			
Validation (2011–2021)*																			
J2000-iso	Cal	Val			RSM			GSM			RSM_biasC								
	Gauges	Upstream	Dam	Down stream	Upstream	Dam	Down stream	Upstream	Dam	Down stream	Upstream	Dam	Down stream	Upstream	Dam	Down stream			
Efficiency	NSE	0.57	0.38	0.73	0.62	0.37	0.75	0.59	0.24	0.59	0.62	0.37	0.71	0.61	0.21	0.68			
	LogNSE	0.68	−1.48	0.73	0.68	−1.62	0.69	0.70	−1.73	0.47	0.77	−1.81	0.69	−0.23	−4.67	0.16			
	Bias	−0.39	−0.09	−0.03	−0.33	4.70E-04	0.06	−0.37	0.20	0.05	−0.36	0.01	0.19	−0.37	0.20	0.03			
	KGE	0.41	0.56	0.80	0.50	0.61	0.86	0.55	0.59	0.78	0.48	0.61	0.74	0.56	0.59	0.82			

Note: \* denotes objective function not included as part of a calibration and used as a validation.

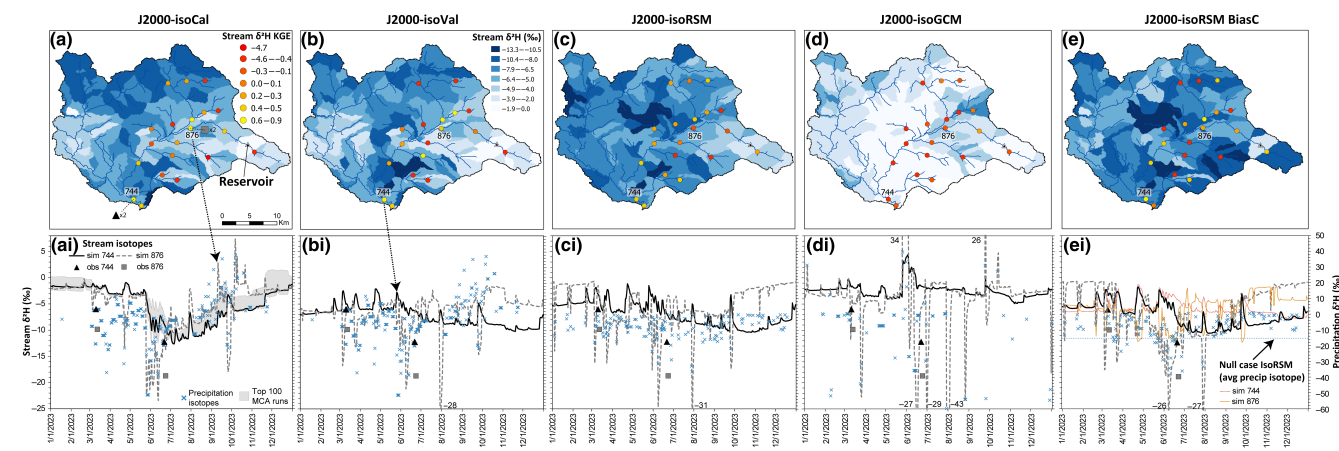


**FIGURE 7** The average simulated stream  $\delta^2\text{H}$  for the sub-basins in the Eerste River using the (a) J2000-isoCal (streamflow and isotope calibration), (b) J2000-isoVal (streamflow calibration only), (c) J2000-isoRSM (streamflow and isotope calibration using isotope data from IsoRSM), (d) J2000-isoGSM (streamflow and isotope calibration using isotope data from IsoGSM) and (e) J2000-isoRSM biasC with both streamflow and isotope calibration using a linear bias corrected IsoRSM as well as calibration with only sensitive parameters, with the stream Kling Gupta efficiency (KGE: Gupta et al., 2009) obtained for each of the measured surface water isotopes. (ai-ei) shows a timeseries plot of simulated stream and precipitation  $\delta^2\text{H}$  compared with measured surface water isotopes for the reach segments 744 and 876 across the different model calibrations. (ai) includes the top 100 Monte Carlo runs from the sensitivity analysis and (ei) includes a null case where the average yearly precipitation isotope composition from IsoRSM was used as the input into J2000-iso for calibration with only sensitive parameters. IsoGSM, isotope-enabled global spectral model; IsoRSM, isotope-enabled regional spectral model.

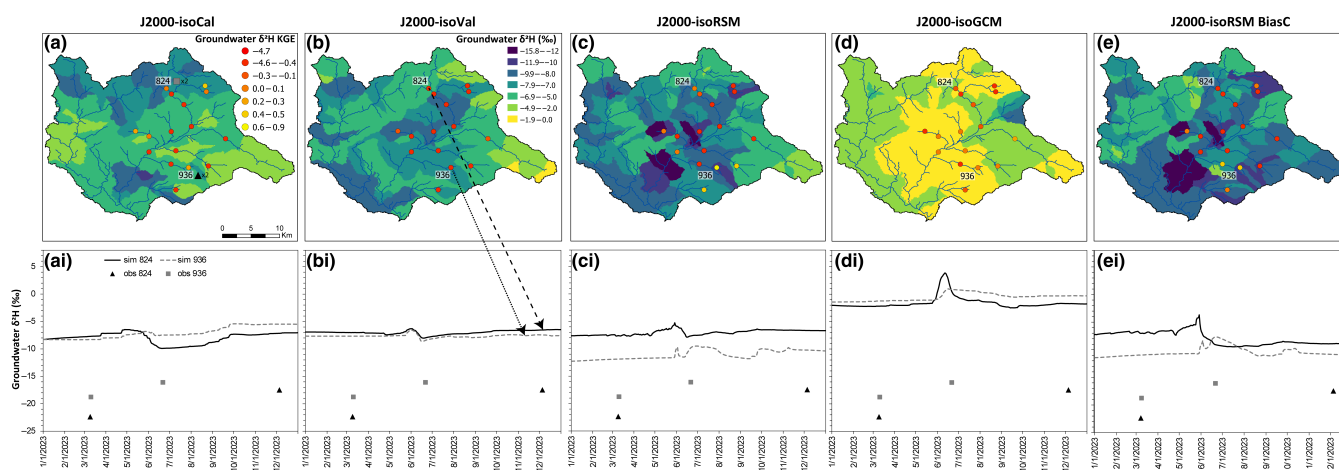


**FIGURE 8** The average simulated groundwater  $\delta^2\text{H}$  (deep groundwater store) for the sub-basins in the Eerste River using the (a) J2000-isoCal (streamflow and isotope calibration) (b) J2000-isoVal (streamflow calibration only), (c) J2000-isoRSM (streamflow and isotope calibration using isotope data from IsoRSM) and (d) J2000-isoGSM (streamflow and isotope calibration using isotope data from IsoGSM) and (e) J2000-isoRSM biasC with both streamflow and isotope calibration using a linear bias corrected IsoRSM as well as calibration with only sensitive parameters, with the groundwater Kling Gupta efficiency (KGE: Gupta et al., 2009) obtained for each of the measured deep groundwater isotopes. (ai-di) shows a timeseries plot of simulated groundwater  $\delta^2\text{H}$  compared with measured groundwater isotopes for the sub-basins 824 and 936 across the different model calibrations. IsoGSM, isotope-enabled global spectral model; IsoRSM, isotope-enabled regional spectral model.

having the minimum and maximum values respectively (Figure 9a-e). Spatially, the simulated ET was similar for J2000-isoCal, J2000-isoVal, J2000-isoRSM, J2000-isoRSM biasC, but J2000-isoGSM had lower simulated ET in the catchment interior. The relative simulated soil saturation across the four models was similar with values between 53%–61%. All the models had a relatively low simulated soil-water saturation (0.1–0.3) in the catchment interior, while the headwaters and western portion of the catchment had higher simulated soil-water

saturation (0.7–0.9). HRUs with complete simulated soil-water saturation were evident in the western portion and center of the catchment; likely a function of slope but also the climate conditions for 2023. The simulated total percolation across each model was different with values ranging from 336 to 627 mm/year (Figure 9ai-ei). J2000-isoCal, J2000-isoRSM and J2000-isoRSM biasC had the most realistic simulated percolation with 32%–39% of precipitation. J2000-isoVal and J2000-GSM had the most simulated percolation

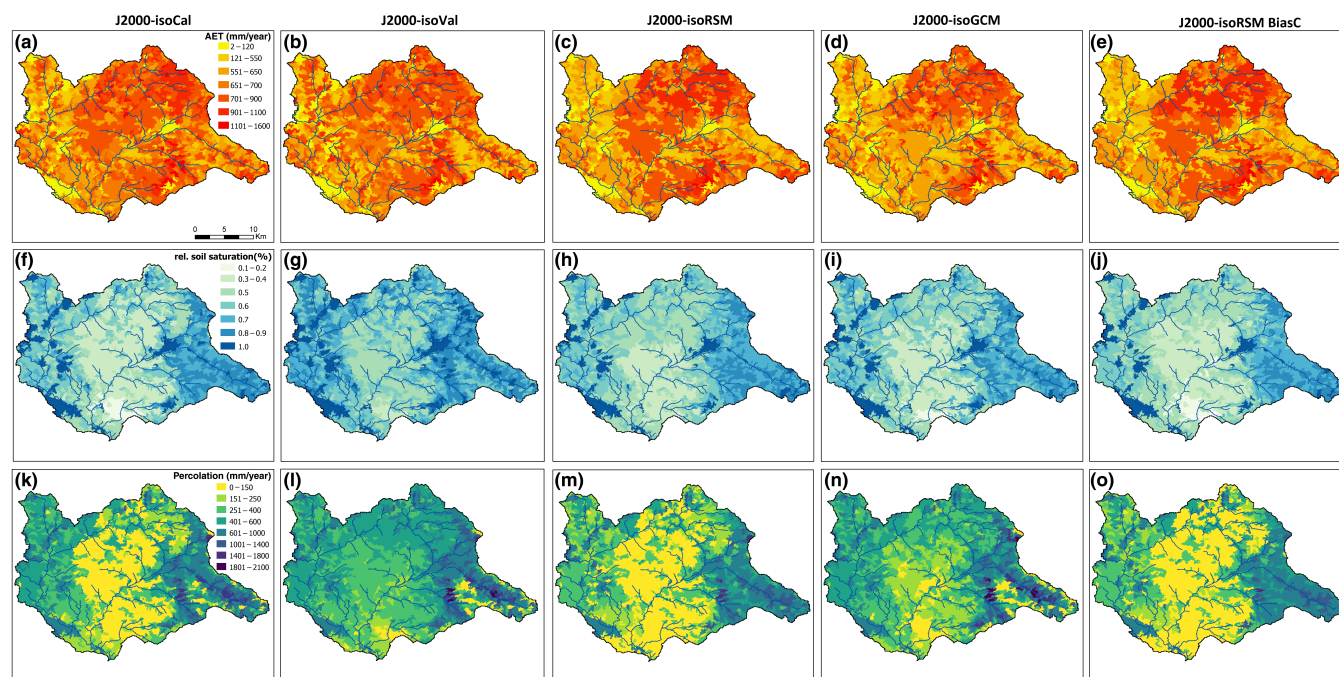


**FIGURE 9** (a–d) The simulated evapotranspiration (mm/year), (e–h) relative soil saturation (average daily %) and (i–l) percolation (mm/year) using the J2000-isoCal (streamflow and isotope calibration), J2000-isoVal (streamflow calibration only), J2000-isoRSM (streamflow and isotope calibration using isotope data from IsoRSM), J2000-isoGSM (streamflow and isotope calibration using isotope data from IsoGSM) and J2000-isoRSM biasC with both streamflow and isotope calibration using a linear bias corrected IsoRSM as well as calibration with only sensitive parameters.

49%–60% and were unlikely to be realistic for the region. Across the models, the most simulated percolation was in the headwaters of the catchment with values more than 1000 mm/year, while the interior and centre of the catchment had percolation values of less than 250 mm/year (Figure 9a–l). J2000-isoVal had the least standard deviation in the simulated percolation between different HRUs, which likely accounted for the higher overall simulated percolation.

For the J2000-isoCal, the scaling parameters for groundwater outflow (RG1\_k and RG2\_k) were the most sensitive across the gauges and for the stream isotopes (Table 4). Parameters regarded as not sensitive and moderately sensitive varied across the different objective functions, but the remaining sensitivity was evenly distributed. The top 100 MCA runs show that during the dry season there was as much as a 5‰ difference in simulated stream  $\delta^2\text{H}$  for reach 744. During the wet season there was a larger difference between the top 100 MCA's with as much as an 8‰ difference in simulated stream  $\delta^2\text{H}$  (Figure 7a).

## 5 | DISCUSSION

### 5.1 | Evaluating isotope-enabled climate models as inputs for J2000-iso




The Eerste River is a small catchment in size (620 km<sup>2</sup>), with a high evaporation demand (1900 mm/year: Schulze, 2008) and spatially

diverse in terms of high and low altitude precipitation (Figure 2b). We used measured precipitation isotopes as a benchmark, two different isotope-enabled climate models, the global IsoGSM (Yoshimura & Kanamitsu, 2008) and the regional IsoRSM (Yoshimura et al., 2010), a bias-corrected IsoRSM to drive the J2000-iso hydrological model. The J2000-iso model driven by IsoRSM and the measured data were similar in terms of streamflow, ET, percolation and stream isotope fit. The stream isotope composition however was impacted by the choice of precipitation isotope data products for J2000-iso. Bias correction of the isotope enabled climate model IsoRSM yielded the best streamflow isotope simulation for J2000-iso (KGE: 0.23 averaged). For the null case, the J2000-iso model parameters dampened the simulated stream isotope composition, but on average were more enriched in heavy isotopes ( $\delta^{18}\text{O}$ ) compared to the bias corrected IsoRSM and had a poor spatial average efficiency across all the sampling points (Table 3). For J2000-iso to achieve good streamflow metrics for the upstream and downstream gauges, the measured climate data were used as a benchmark opposed to the climate data from IsoRSM and IsoGSM. Comparing measured with climate model data, IsoRSM simulated 232 days of no precipitation as opposed to the observed data of 95. The measured precipitation exhibited 180 days with small events (0–2 mm), compared with only 60 and 10 days for IsoRSM and IsoGSM, respectively.

We tested several simulations using the precipitation amounts of IsoRSM and IsoGSM applying 3.5 times and 2.5 times linear yearly bias correction, respectively. But the downstream dynamics in the

**TABLE 4** Results of the Monte Carlo analysis (MCA) used to understand the relative sensitivity of the different model parameters using the Nash–Sutcliffe efficiency NSE (Nash, 1970), LogNSE and Kling Gupta efficiency KGE (Gupta et al., 2009) as objective function for the upstream gauging station Jonkershoek (calibration point), outflow from the Kleinplaas reservoir (validation only), the downstream gauging station Klein Welmoed and spatial efficiency attained for the stream isotopes.

Number	Name of parameter	J2000-isoCal							
		Upstream		Reservoir	Downstream		Stream-iso	RG1-iso	RG2-iso
		NSE	LogNSE	KGE	NSE	LogNSE	KGE	KGE	KGE
1	AC_Adaptation	0.03	0.03	0.04	0.05	0.03	0.02	0.1	0.04
2	FC_Adaptation	0.03	0.03	0.02	0.03	0.04	0.05	0.09	0.03
3	soilConcRD1	0.04	0.05	0.02	0.02	0.08	0.04	0.08	0.02
4	soilConcRD2	0.03	0.03	0.03	0.02	0.04	0.03	0.03	0.02
5	SoilLatVertDist	0.03	0.03	0.05	0.03	0.02	0.05	0.06	0.03
6	soilLinRed	0.03	0.05	0.02	0.02	0.04	0.02	0.03	0.03
7	soilMaxPerc	0.04	0.03	0.05	0.02	0.02	0.04	0.04	0.02
8	soilOutLPS	0.04	0.07	0.05	0.02	0.02	0.05	0.02	0.04
9	flowrouteTA	0.03	0.05	0.03	0.05	0.03	0.02	0.03	0.02
10	RG1RG2max	0.03	0.03	0.03	0.06	0.04	0.03	0.07	0.02
11	RG1_k	0.05	0.33	0.03	0.03	0.05	0.07	0.32	0.05
12	RG2_k	0.53	0.18	0.58	0.61	0.53	0.53	0.04	0.6
14	IsoMixHruReach	0.04	0.04	0.02	0.02	0.02	0.03	0.03	0.03
15	IsoMixProp	0.04	0.03	0.03	0.03	0.03	0.03	0.05	0.03

Note: Sensitivity:  high;  moderate;  Low.

simulated runoff became purely synthetic when using IsoRSM and IsoGSM precipitation volumes, due to the larger noise-to-signal ratio for these small (<2 mm) events. Such issues were also found in Watson, Kralisch, et al. (2024) and Arciniega-esparza et al. (2023) but measured precipitation volumes were not available for further testing. Climate Hazards Group InfraRed Precipitation (CHIRPS: Funk et al., 2015) has also been used as input data for rainfall-runoff models in catchments in South Africa (du Plessis & Kibii, 2021; Kibii & du Plessis, 2024) and while bias has been noted, impacts to hydrological process simulations have not been fully explored and could also be associated with the sensitivity of certain parameters in J2000. In contrast to the precipitation volumes from IsoGSM and IsoRSM, the precipitation isotopes resulted in good stream isotope fits across several sites within the basin. A monthly linear correction improved the stream isotope fit considerably and this is recommended for future applications of IsoGSM and IsoRSM (i.e., Arciniega-esparza et al., 2023). To improve the application of isotope-enabled models it would be beneficial to feed additional local meteorological records and measured isotope precipitation compositions over and above the existing reanalysis correction used by the climate models. Furthermore, an application of J2000-iso for a small 1–2km<sup>2</sup> catchment could test the benefits of including isotopes in developing more robust hydrological models. The streamflow isotopes for the Eerste were well mixed and showed a variation of 4‰ for  $\delta^2\text{H}$ , but were barely larger than the analytical precision of around 0.5‰ for  $\delta^2\text{H}$  (Mattei

et al., 2021) and further testing of input data, isotope mixing and fractionation components are still required.

A comparison of the impact of driving isotope-enabled hydrological models with different precipitation isotope data on simulated streamflow and stream isotopes, has previously been performed in Canada and Tibetan Plateau (Delavau et al., 2017; Nan et al., 2021). Similar to our application using J2000-iso, they compared an isotope-enabled climate model (REMOiso: Sturm et al., 2005) with different static and low temporal precipitation isotope inputs to drive the isotope-enabled rainfall-runoff model IsoWATFLOOD (Stadnyk et al., 2013). Like this Canadian application, which was applied for a meso-scale catchment (1300 km<sup>2</sup>) and with snow as a significant source of precipitation (35%–40%), the choice of isotope precipitation data had more impact on the stream isotope fit than the overall simulated water balance. The testing of different measured climate data was not explored by Delavau et al. (2017) but is likely less of an issue for the climate and overall catchment size that was used.

Given that many countries do not have enough precipitation isotope data to build isotope-enabled models, global reanalysis products such as IsoGSM, IsoRSM, REMOiso and machine learning approaches such as PISOAI (available for Europe: Nelson et al., 2021) are essential in building more robust models, capturing streamflows for ungauged basins and simulating a wider range of hydrological processes. Additionally, the development of new global reanalysis precipitation isotope products is an essential next step for improving the uptake of

isotope-enabled modelling and the associated benefits from more stringent model evaluation.

## 5.2 | Improving sample collection for evaluation of isotope-enabled rainfall-runoff models

Isotope sample collection methods for rain, stream and groundwater are still manual sampling, or (budget allowing) with automated samplers (Ankor et al., 2019; Michelsen et al., 2019). While manual sampling and recommended guidelines for sample collection are extensive for isotope hydrological studies (International Atomic Energy Agency, 2005, 2008), recommendations of sample collection principles for isotope-enabled models are limited. In this study we followed a manual collection regime where the target number of rainfall, groundwater and stream water collection sites was dependent on access to local farms, proximity of the river to access roads and the willingness of land-owners to collect rainwater during precipitation events. Using this approach there was an oversampling of stream and groundwater in comparison to precipitation even though precipitation is the key input (Birkel et al., 2020). In contrast to others studies, where precipitation isotopes were spatially homogenous (Smith et al., 2021; Wu et al., 2022), our study showed high spatial and temporal variability. This resulted in the model only capturing the stream isotope compositions for the main channel of the Eerste (Figure 7). Likewise, all the models showed enrichment of heavy isotopes after the inclusion of outflow from the reservoir, as a result of fractionation from the surface water. The precipitation collection did not capture the spatial variability of precipitation isotopes, and hence, smaller tributaries could not be well simulated. The model also presented a higher performance for stream isotopes when the nearest neighbour interpolation method was used, in contrast with the inverse distance weight method which has shown good performance for measured precipitation amounts with dense station networks (Dirks et al., 2002). The limited number of precipitation collection sites also meant that if a specific precipitation event was not collected, then the nearest stream isotope composition could not be simulated. The usability of data from manual collection of precipitation is dependent on the date stamp matching the actual events recorded by the local weather stations. The presupposition that the last known daily cumulative precipitation isotope composition, is still relevant for days with missed events is a method we used to ensure that isotope transport was not halted by a date stamp mismatch between collection and weather station records.

Like stream water collection, the groundwater collection sites exceeded the rainfall collection sites. The isotope variability in the deep groundwater was greater than that in the stream. Given that the groundwater isotope variability is normally dampened due to flow mixing, this represents a conceptually challenging situation to simulate. For this reason, careful selection of deep groundwater collection sites should be done to use groundwater isotopes for validation or calibration of the model. The inclusion of water level monitoring as part of the application of isotope or tracer-aided model data collection, is necessary to ensure groundwater sampling points are only

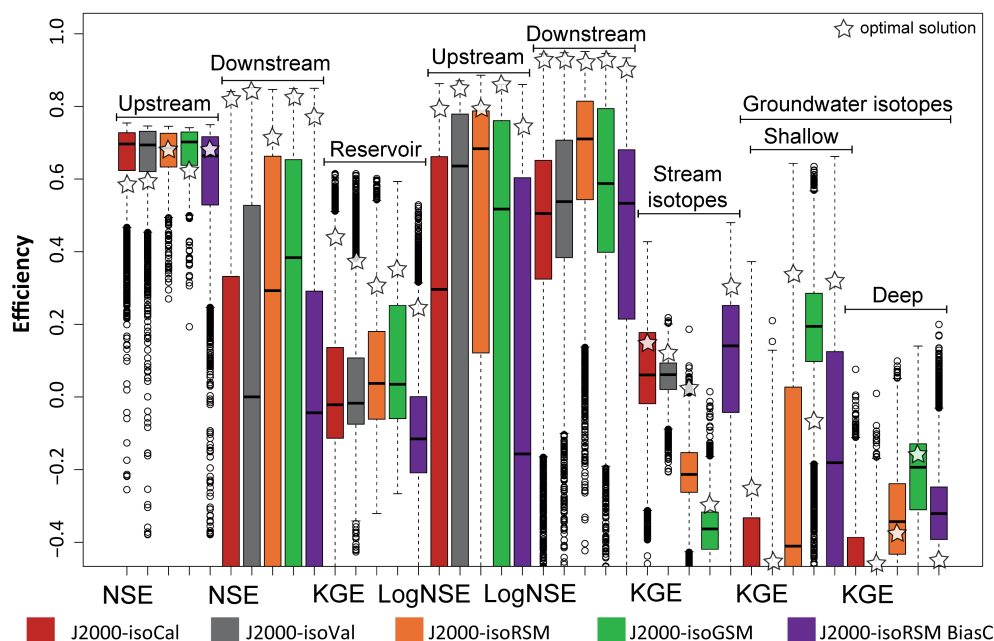
influenced by vertically percolating rainwater, conform to methods of recharge calculation such as the water level fluctuation method (Crosbie et al., 2005), as other groundwater flow complexities are not considered by J2000-iso and conventional rainfall-runoff models. Complex groundwater flow and the flow of groundwater through fault systems are common features of regions like the Eerste River and add additional complexity in simulating the groundwater system and regional groundwater recharge (Conrad et al., 2004; Watson et al., 2018; Watson et al., 2020). Prioritization of higher resolution sampling is recommended in catchments with a high spatial precipitation variability (Birkel et al., 2011). Given that the Eerste River and the Jonkershoek have an existing network of reliable climate and stream-flow gauging stations, the continuation of isotope monitoring in this catchment is recommended to improve the development of components needed in isotope-enabled modelling.

## 5.3 | Simulating potential groundwater recharge with isotope-enabled models

The simulation of percolation using rainfall-runoff models is the potential amount of rain water that contributes to the groundwater system but does not consider aquifer storage and other hydraulic parameters (Scanlon et al., 2002; Watson et al., 2018). An overestimation of percolation has implications for the potential to capture groundwater isotope compositions and dynamics. A high percolation would result in a higher simulated groundwater isotope dynamic, but also enhance the overall heavy isotope enrichment. Of the five models tested in this study, J2000 driven by a bias-corrected isoRSM performed the best in terms of the deep and shallow groundwater isotope compositions (Figure 10). While the limitations of groundwater components in J2000 impact realistic simulations of percolation, the calibration during the second wettest year in 29 years resulted in an overestimation of long-term percolation. We found, however, that the simulated percolation rate of 19% during the validation of a dry year (2003) matched the midpoint between literature-based recharge estimates of the TMG (13%–27% of MAP: Weaver & Talma, 2005; Wu & Xu, 2005; Miller et al., 2017; Watson et al., 2019).

The dominance of large precipitation events in recharging aquifers is well documented and supports a higher estimation of recharge during wet years (Jasechko & Taylor, 2015; Taylor et al., 2013). Our model estimates are, however, much larger than recharge estimates for the local alluvial aquifer (2%–5.6% of MAP) (Conrad et al., 2004; Watson et al., 2020). Compared with the standard J2000 model, the simulated percolation of J2000-iso is more realistic and recommended when driving J2000 with any projections of the future climate. The overestimation of percolation by many rainfall-runoff models for catchments with a Mediterranean climate and a high proportion of yearly precipitation during winter, such as the Eerste River, influences the selection of viable climate change adaptation options. The need to improve the simulation of groundwater recharge within rainfall-runoff models is important given declining recharge amounts and aquifer water levels globally (i.e., Jasechko et al., 2024).

**FIGURE 10** A box and whisker plot showing the solution efficiencies Nash Sutcliffe efficiency (NSE) in standard form; Nash, 1970, logarithmic form: logNSE and the Kling Gupta efficiency: KGE, Gupta et al., 2009) from J2000-isoCal, J2000-isoVal, J2000-isoRSM and J2000-isoGSM, J2000-isoRSM BiasC for the upstream, downstream and reservoir gauge as well as the stream isotopes and groundwater isotopes.



## 5.4 | Isotope-enabled rainfall-runoff modelling for improved water management

Comparison of isotope-enabled models with non-isotope enabled models for the Eerste River in this study but also the San Carlos catchment in Costa Rica (Watson, Kralisch, et al., 2024) using J2000-iso have demonstrated the added value of integrating isotope tracers. In both studies non-isotope enabled models showed a disparity between the amounts of simulated percolation. For Costa Rica, a higher percolation was simulated by the isotope-enabled model compared with a non-isotope enabled model. The opposite occurred in the Eerste River, with the isotope-enabled model reducing the overall simulated percolation compared with a non-isotope enabled model. Since percolation represents the transfer of surface water into long-term underground storage, its accurate estimation is a critical piece of information needed by water managers to adapt to climate change. Specifically, climate change adaption strategies to improve the allocation of water used for irrigation, hydropower generation, flood protection as well as in the development of drought relief options are impacted by realistic quantification of percolation within these two applications of the J2000-iso. For over six decades, the GNIP has been collecting monthly data and this serves as an invaluable resource that allows initial calibration and validation during the setup of isotope-enabled hydrological models. However, to extract the full value of the information generated by isotope-enabled models, catchment specific sub-monthly and ideally daily monitoring of precipitation is required to generate the necessary isotope datasets. In this study we have shown that simulated data from isotope-enabled climate models can provide the necessary input data to run isotope-enabled hydrological models and this is not restricted to just the J2000-iso. Expanding

the availability and access to simulated isotope data from climate models is essential to broaden the use of isotope enabled hydrological models. However, in times of declining monitoring networks (Wohl et al., 2012, for an example from the tropics), the collection of observed data is required so that these models can be evaluated. A direct coupling of isotope-enabled climate models with isotope enabled hydrological models is a valuable next step to integrate feedback between atmospheric and hydrological conditions and improve the simulation of vapour isotope fluxes.

## 6 | CONCLUSION

Isotope-enabled climate models offer the potential to increase the use of their counterpart hydrological models in the generation of more robust simulations of climate, hydrology and environmental conditions. The generation of robust simulations is becoming increasingly important considering climate change impacts such as increasing water scarcity, melting glaciers and the re-occurrence of extreme events. The regional version of the isotope-enabled climate model considers more local conditions and is better suited for input into rainfall-runoff modelling but requires long lead-times for data generation. In smaller catchments, which are spatially diverse in terms of high and low altitude precipitation, using only the isotope precipitation data from the regional climate model (IsoRSM) offers the potential to capture both stream isotope variability but also streamflow amounts. The continued collection of isotope data is still necessary to bias correct inputs as well as validate and calibrate hydrological models. Whilst manual collection of isotope data is widely used in developing countries as inputs into isotope-enabled models, the data often require temporal alignment with the other locally collected climate

data. The sampling and collection of precipitation isotope data should have the highest priority when setting up a sample collection plan for catchments with spatially diverse precipitation patterns. In situations where the sampled groundwater exhibits a higher-than-expected spatial isotope variability, compared with stream water, careful selection of validation/calibration points is required. Even though scarce isotope data limits long-term calibration and validations of rainfall-runoff models, a single year's calibration with an isotope-enabled model can still yield good model robustness and hydrological process simulation. The development of more robust hydrological simulations is important when identifying risks associated to extreme events as well as the effectiveness of climate change adaption strategies. A first step in this process would be coupling of the isotope-enabled climate and hydrological models to better capture linkages between atmospheric and hydrological conditions and how these links evolve in response to climate change.

## ACKNOWLEDGEMENTS

This article was funded by: the European Union under the grant agreement No GA 101082048 (MAR2PROTECT project), UNESCO project title "Climate Risk Management in South African Biosphere Reserves" (contract 4500461954), the Water Research Commission (C2024/205-01587) and International Atomic Energy Agency CRP 31004. CB acknowledges support through the Leibniz Institute of Freshwater Ecology and Inland Fisheries (IGB) in Berlin. The field sampling was made possible by the landowners of Stellenbosch who collected rainfall samples as well as permitted access to their properties and boreholes. We would like to thank the editor in chief and two anonymous reviewers for their valuable comments and feedback which improved this paper. The views and opinions expressed here are those of the author(s) only and do not necessarily reflect those of the European Union nor the granting authority, which cannot be held responsible for them.

## DATA AVAILABILITY STATEMENT

The data that support the findings of this study are available on request from the corresponding author. The data are not publicly available due to privacy or ethical restrictions.

## ORCID

Andrew Watson  <https://orcid.org/0000-0001-5998-6933>

Christian Birkel  <https://orcid.org/0000-0002-6792-852X>

Saul Arciniega-Esparza  <https://orcid.org/0000-0002-1064-5692>

Jan de Waal  <https://orcid.org/0000-0001-8034-7538>

Jodie Miller  <https://orcid.org/0000-0003-2290-3932>

Yuliya Vystavna  <https://orcid.org/0000-0002-1366-0767>

Jared van Rooyen  <https://orcid.org/0000-0002-0898-4791>

Angela Welham  <https://orcid.org/0000-0001-6961-5319>

Kei Yoshimura  <https://orcid.org/0000-0002-5761-1561>

Jörg Helmschrot  <https://orcid.org/0000-0002-4756-7640>

Annika Künne  <https://orcid.org/0000-0002-4925-0882>

Sven Kralisch  <https://orcid.org/0000-0003-2895-540X>

## REFERENCES

- Amer, K. H., & Hatfield, J. L. (2004). Canopy resistance as affected by soil and meteorological factors in potato. *Agronomy Journal*, 96(4), 978–985. <https://doi.org/10.2134/agronj2004.0978>
- Ankor, M. J., Tyler, J. J., & Hughes, C. E. (2019). Development of an autonomous, monthly and daily, rainfall sampler for isotope research. *Journal of Hydrology*, 575, 31–41.
- Arciniega-esparza, S., Birkel, C., Durán-quesada, A. M., Moore, G. W., Maneta, M. P., Sánchez-murillo, R., Negri, L. B., Tetzlaff, D., & Soulsby, C. (2023). Tracer-aided ecohydrological modelling across climate, land cover, and topographical gradients in the tropics. *Hydrological Processes*, 37(5), e14884. <https://doi.org/10.1002/hyp.14884>
- Batjes, N., Dijkshoorn, K., van Engelen, V., Fischer, G., Jones, A., Montanarella, L., Petri, M., Prieler, S., Teixeira, E., Wiberg, D., & Shi, X. (2012). Harmonized world soil database. Rome.
- Birkel, C., Correa-Barahona, A., Martínez-Martínez, M., Granados-Bolaños, S., Venegas-Cordero, N., Gutiérrez-García, K., Blanco-Ramírez, S., Quesada-Mora, R., Solano-Rivera, V., Mussio-Mora, J., Chavarría-Palma, A., Vargas-Arias, K., Moore, G. W., Durán-Quesada, A. M., Vasquez-Morera, J., Soulsby, C., Tetzlaff, D., Espinoza-Cisneros, E., & Sánchez-Murillo, R. (2020). Headwaters drive streamflow and lowland tracer export in a large-scale humid tropical catchment. *Hydrological Processes*, 34(18), 3824–3841. <https://doi.org/10.1002/hyp.13841>
- Birkel, C., Helliwell, R., Thornton, B., Gibbs, S., Cooper, P., Soulsby, C., Tetzlaff, D., Spezia, L., Esquivel-Hernández, G., Sánchez-Murillo, R., & Midwood, A. J. (2018). Characterization of surface water isotope spatial patterns of Scotland. *Journal of Geochemical Exploration*, 194, 71–80. <https://doi.org/10.1016/j.gexplo.2018.07.011>
- Birkel, C., & Soulsby, C. (2015). Advancing tracer-aided rainfall-runoff modelling: A review of progress, problems and unrealised potential. *Hydrological Processes*, 29(25), 5227–5240.
- Birkel, C., Tetzlaff, D., Dunn, S. M., & Soulsby, C. (2011). Using time domain and geographic source tracers to conceptualize streamflow generation processes in lumped rainfall-runoff models. *Water Resources Research*, 47(2), W02515.
- Bong, H., Cauquoin, A., Okazaki, A., Chang, E., Werner, M., Wei, Z., Yeo, N., & Yoshimura, K. (2024). Process-based intercomparison of water isotope-enabled models and reanalysis nudging effects. *Journal of Geophysical Research: Atmospheres*, 129(1), e2023JD038719.
- Conrad, J., Nel, J., & Wentzel, J. (2004). The challenges and implications of assessing groundwater recharge: A case study—Northern Sandveld, Western cape, South Africa. *Water SA*, 30(5), 75–81. <https://doi.org/10.3390/jerph8062418>
- Conrad, J., Smit, L., Murray, K., van Gend-Muller, J., & Seyler, H. (2019). The Malmesbury group—an aquifer of surprising significance. *South African Journal of Geology*, 122(3), 331–342. <https://doi.org/10.25131/sajg.122.0028>
- Craig, H., & Gordon, L. I. (1965). Deuterium and oxygen-18 variations in the ocean and the marine atmosphere. In E. Tongiorgi (Ed.), *Stable iso&hyphen; topes in oceanographic studies and palaeotemperatures* (pp. 9–130). Lab Geologia Nucleare.
- Crosbie, R. S., Binning, P., & Kalma, J. D. (2005). A time series approach to inferring groundwater recharge using the water table fluctuation method. *Water Resources Research*, 41(1), 1–9. <https://doi.org/10.1029/2004WR003077>
- Dansgaard, W. (1964). Stable isotopes in precipitation. *Tellus*, 16(4), 436–468. <https://doi.org/10.3402/tellusa.v16i4.8993>
- Deb, K., Pratap, A., Agarwal, S., & Meyarivan, T. (2002). A fast and elitist multiobjective genetic algorithm: NSGA-II. *IEEE Transactions on Evolutionary Computation*, 6(2), 182–197. <https://doi.org/10.1109/4235.996017>
- Delavau, C. J., Stadnyk, T., & Holmes, T. (2017). Examining the impacts of precipitation isotope input ( $\delta^{18}\text{O}$  ppt) on distributed, tracer-aided

- hydrological modelling. *Hydrology and Earth System Sciences*, 21(5), 2595–2614.
- Dirks, K., Hay, J., Stow, C. D., & Harris, D. (2002). High-resolution studies of rainfall on Norfolk Island. Part IV: Observations of fractional time raining. *Journal of Hydrology*, 263(1–4), 156–176. [https://doi.org/10.1016/S0022-1694\(02\)00057-4](https://doi.org/10.1016/S0022-1694(02)00057-4)
- du Plessis, K. D., & Kibii, J. (2021). Applicability of CHIRPS-based satellite rainfall estimates for South Africa. *Journal of the South African Institution of Civil Engineering*, 63(3), 43–54. Available at: <https://www.scopus.com/inward/record.uri?eid=2-s2.0-85121775024&doi=10.17159%2F2309-8775%2F2021%2Fv63n3a4&partnerID=40&md5=05395595daed72db9528e62cca4c70f8>
- Funk, C., Peterson, P., Landsfeld, M., Pedreros, D., Verdin, J., Shukla, S., Husak, G., Rowland, J., Harrison, L., Hoell, A., & Michaelsen, J. (2015). The climate hazards infrared precipitation with stations—a new environmental record for monitoring extremes. *Scientific Data*, 2(1), 1–21. Available at: <https://www.scopus.com/inward/record.uri?eid=2-s2.0-84961120091&doi=10.1038%2Fsd2015.66&partnerID=40&md5=d94ac51fea6314b27c45c55128a23b05>
- GeoTerralimage. (2015). 2013–2014 South African National Land-Cover Dataset.
- Gudmundsson, L., Bremnes, J. B., Haugen, J. E., & Engen-Skaugen, T. (2012). Technical note: Downscaling RCM precipitation to the station scale using statistical transformations – a comparison of methods. *Hydrology and Earth System Sciences*, 16(9), 3383–3390. <https://doi.org/10.5194/hess-16-3383-2012>
- Gupta, H. V., Kling, H., Yilmaz, K. K., & Martinez, G. F. (2009). Decomposition of the mean squared error and NSE performance criteria: Implications for improving hydrological modelling. *Journal of Hydrology*, 377(1–2), 80–91. <https://doi.org/10.1016/j.jhydrol.2009.08.003>
- Herrmann, A., & Stichler, W. (1981). Runoff modeling using environmental isotopes. *On Water and Nutrient Simulation Models*, 4, 41.
- Hersbach, H., Bell, B., Berrisford, P., Hirahara, S., Horányi, A., Muñoz-Sabater, J., Nicolas, J., Peubey, C., Radu, R., Schepers, D., Simmons, A., Soci, C., Abdalla, S., Abellan, X., Balsamo, G., Bechtold, P., Biavati, G., Bidlot, J., Bonavita, M., ... Thépaut, J.-N. (2020). The ERA5 global reanalysis. *Quarterly Journal of the Royal Meteorological Society*, 146(730), 1999–2049. <https://doi.org/10.1002/qj.3803>
- Holmes, T. L., Stadnyk, T. A., Asadzadeh, M., & Gibson, J. J. (2023). Guidance on large scale hydrologic model calibration with isotope tracers. *Journal of Hydrology*, 621, 129604. <https://doi.org/10.1016/j.jhydrol.2023.129604>
- Horita, J., & Wesolowski, D. J. (1994). Liquid-vapor fractionation of oxygen and hydrogen isotopes of water from the freezing to the critical temperature. *Geochimica et Cosmochimica Acta*, 58(16), 3425–3437.
- Hornberger, G. M., & Spear, R. C. (1981). An approach to the preliminary analysis of environmental systems. *Journal of Environmental Management*, 12(1), 7–18.
- IAEA. (2022). *Towards best practices in isotope-enabled hydrological modelling applications final report of a coordinated research project*. IAEA.
- International Atomic Energy Agency. (2005). *Isotopic composition of precipitation in the Mediterranean basin in relation to air circulation patterns and climate*. International Atomic Energy Agency.
- International Atomic Energy Agency. (2008). *Global network of isotopes in precipitation (GNIP)*. IAEA.
- Jasechko, S., Seybold, H., Perrone, D., Fan, Y., Shamsudduha, M., Taylor, R. G., Fallatah, O., & Kirchner, J. W. (2024). Rapid groundwater decline and some cases of recovery in aquifers globally. *Nature*, 625(7996), 715–721. <https://doi.org/10.1038/s41586-023-06879-8>
- Jasechko, S., Sharp, Z. D., Gibson, J. J., Birks, S. J., Yi, Y., & Fawcett, P. J. (2013). Terrestrial water fluxes dominated by transpiration. *Nature*, 496(7445), 347–350.
- Jasechko, S., & Taylor, R. G. (2015). Intensive rainfall recharges tropical groundwaters. *Environmental Research Letters*, 10(12), 124015. <https://doi.org/10.1088/1748-9326/10/12/124015>
- Johnson, M., & Thamm, A. (2006). The cape supergroup. In M. R. Johnson, C. R. Anhaeusser, & R. J. Thomas (Eds.), *The geology of South Africa* (pp. 443–459). Geological Society of South Africa.
- Johnson, P. A. (1983). *Variations in albedo among natural and disturbed South Western Cape veld types*. University of Cape Town.
- Kibii, J. K., & du Plessis, J. A. (2024). Applicability of CHIRPS-based Pitman model for simulation of climate change flows. *Physics and Chemistry of the Earth, Parts A/B/C*, 135, 103643. <https://doi.org/10.1016/j.pce.2024.103643>
- Koeniger, P., Stumpp, C., & Schmidt, A. (2022). Stable isotope patterns of German rivers with aspects on scales, continuity and network status. *Isotopes in Environmental and Health Studies*, 58(4–6), 363–379. <https://doi.org/10.1080/10256016.2022.2127702>
- Kralisch, S., & Krause, P. (2006). JAMS—A framework for natural resource model development and application. In A. Voinov, A. Jakeman, & A. E. Rizzoli (Eds.), *Proceedings of the iEMSs 3rd biennial meeting* (pp. 6–11). Summit on Environmental Modelling and Software. <https://scholarsarchive.byu.edu/iemssconference/2006/all/9>
- Krause, P. (2001). *Das hydrologische Modellsystem J2000-Beschreibung und Anwendung in großen Flußgebieten*. Programmgruppe Systemforschung und Technologische Entwicklung.
- Krause, P., & Kralisch, S. (2005). The hydrological modelling system J2000—Knowledge core for JAMS. In A. Zerger & R. M. Argent (Eds.), *Proceedings of the MODSIM 2005 international congress on modelling and simulation* (pp. 676–682).
- Kuppel, S., Tetzlaff, D., Maneta, M. P., & Soulsby, C. (2018). EcH2O-iso 1.0: Water isotopes and age tracking in a process-based, distributed ecohydrological model. *Geoscientific Model Development*, 11(7), 3045–3069. <https://doi.org/10.5194/gmd-11-3045-2018>
- Lynch, S. (2004). *Development of a raster database of annual, monthly and daily rainfall for southern Africa*. Water Research Commission.
- Mattei, A., Huneau, F., Garel, E., Santoni, S., & Vystavna, Y. (2021). Evaporation in Mediterranean conditions: Estimations based on isotopic approaches at the watershed scale. *Hydrological Processes*, 35(5), e14085. <https://doi.org/10.1002/hyp.14085>
- Michelsen, N., Laube, G., Friesen, J., Weise, S. M., Said, A. B. A. B., & Müller, T. (2019). Technical note: A microcontroller-based automatic rain sampler for stable isotope studies. *Hydrology and Earth System Sciences*, 23(6), 2637–2645. <https://doi.org/10.5194/hess-23-2637-2019>
- Miller, J. A., Dunford, A. J., Swana, K. A., Palcsu, L., Butler, M., & Clarke, C. E. (2017). Stable isotope and noble gas constraints on the source and residence time of spring water from the Table Mountain Group Aquifer, Paarl, South Africa and implications for large scale abstraction. *Journal of Hydrology*, 551, 100–115. <https://doi.org/10.1016/j.jhydrol.2017.05.036>
- Miller, J. A., Turner, K. B., Watson, A., van Rooyen, J., Molnár, M., Türi, M., & Palcsu, L. (2022). Characterization of groundwater types and residence times in the Verlorenvlei catchment, South Africa to constrain recharge dynamics and hydrological resilience. *Journal of Hydrology*, 613(August), 128280. <https://doi.org/10.1016/j.jhydrol.2022.128280>
- Miller, J. A., Watson, A. P., Fleischer, M., Eilers, A., Sigidi, N. T., van Gend, J., van Rooyen, J. D., Clarke, C. E., & de Clercq, W. P. (2018). Groundwater quality, quantity, and recharge estimation on the West Coast of South Africa. In R. Revermann, K. M. Krewenka, U. Schmiedel, J. Olwoch, J. Helmschrot, & N. Jürgens (Eds.), *In: Climate change and adaptive land management in southern Africa—assessments, changes, challenges, and solutions* (pp. 86–95). Klaus Hess Publishers. <https://doi.org/10.7809/b-e.00309>
- Munitz, S., Netzer, Y., & Schwartz, A. (2017). Sustained and regulated deficit irrigation of field-grown merlot grapevines. *Australian Journal of Grape and Wine Research*, 23(1), 87–94. <https://doi.org/10.1111/ajgw.12241>
- Nan, Y., He, Z., Tian, F., Wei, Z., & Tian, L. (2021). Can we use precipitation isotope outputs of isotopic general circulation models to improve

- hydrological modeling in large mountainous catchments on the Tibetan plateau? *Hydrology and Earth System Sciences*, 25(12), 6151–6172. <https://doi.org/10.5194/hess-25-6151-2021>
- Nan, Y., Tian, L., He, Z., Tian, F., & Shao, L. (2021). The value of water isotope data on improving process understanding in a glacierized catchment on the Tibetan plateau. *Hydrology and Earth System Sciences*, 25(6), 3653–3673. <https://doi.org/10.5194/hess-25-3653-2021>
- Nash, J. E. (1970). River flow forecasting through conceptual models, I: A discussion of principles. *Journal of Hydrology*, 10, 398–409.
- Nelson, D. B., Basler, D., & Kahmen, A. (2021). Precipitation isotope time series predictions from machine learning applied in Europe. *Proceedings of the National Academy of Sciences*, 118(26), e2024107118.
- Penman, H. L. (1948). Natural evaporation from open water, bare soil and grass. *Proceedings of the Royal Society of London Series A. Mathematical and Physical Sciences*, 193(1032), 120–145.
- Pfennig, B., Kipka, H., Wolf, M., Fink, M., Krause, P., & Flügel, W. A. (2009). Development of an extended routing scheme in reference to consideration of multi-dimensional flow relations between hydrological model entities. In R. Anderssen, R. Braddock, & L. Newham (Eds.), *Proceedings of the 18th World IMACS congress and MODSIM09 international congress on modelling and simulation* (pp. 1972–1978). IAHS-AISH Publication.
- Roffe, S. J., Fitchett, J. M., & Curtis, C. J. (2019). Classifying and mapping rainfall seasonality in South Africa: A review. *South African Geographical Journal*, 101(2), 158–174. <https://doi.org/10.1080/03736245.2019.1573151>
- Scanlon, B. R., Healy, R. W., & Cook, P. G. (2002). Choosing appropriate techniques for quantifying groundwater recharge. *Hydrogeology Journal*, 10(1), 18–39. <https://doi.org/10.1007/s10040-001-0176-2>
- Schaap, M. G., Leij, F. J., & Van Genuchten, M. T. (2001). Rosetta: A computer program for estimating soil hydraulic parameters with hierarchical pedotransfer functions. *Journal of Hydrology*, 251(3–4), 163–176. [https://doi.org/10.1016/S0022-1694\(01\)00466-8](https://doi.org/10.1016/S0022-1694(01)00466-8)
- Schulze, R. E. (2008). *South African atlas of climatology and Agrohydrology* [electronic resource]. Pretoria.
- Simunek, J., Van Genuchten, M. T., & Sejna, M. (2011). The HYDRUS software package for simulating the two- and three-dimensions movement of water, heat, and multiple solutes in variably-saturated media. *Technical Manual*, 230.
- Smith, A., Tetzlaff, D., Kleine, L., Maneta, M., & Soulsby, C. (2021). Quantifying the effects of land use and model scale on water partitioning and water ages using tracer-aided ecohydrological models. *Hydrology and Earth System Sciences*, 25(4), 2239–2259. <https://doi.org/10.5194/hess-25-2239-2021>
- SRK. (2009). Preliminary assessment of impact of the proposed Riviera tungsten mine on groundwater resources preliminary assessment of impact of the proposed Riviera tungsten mine on groundwater resources.
- Stadnyk, T. A., Delavau, C., Kouwen, N., & Edwards, T. W. D. (2013). Towards hydrological model calibration and validation: Simulation of stable water isotopes using the isoWATFLOOD model. *Hydrological Processes*, 27(25), 3791–3810. <https://doi.org/10.1002/hyp.9695>
- Sturm, K., Hoffmann, G., Langmann, B., & Stichler, W. (2005). Simulation of  $\delta^{18}\text{O}$  in precipitation by the regional circulation model REMOiso. *Hydrological Processes*, 19(17), 3425–3444.
- Taylor, R. G., Scanlon, B., Döll, P., Rodell, M., Van Beek, R., Wada, Y., Longuevergne, L., Leblanc, M., Famiglietti, J. S., Edmunds, M., Konikow, L., Green, T. R., Chen, J., Taniguchi, M., Bierkens, M. F. P., MacDonald, A., Fan, Y., Maxwell, R. M., Yechieli, Y., ... Treidel, H. (2013). Ground water and climate change. *Nature Climate Change*, 3(4), 322–329. <https://doi.org/10.1038/nclimate1744>
- Theron, J. N. (1990). *Geological map 3318 Cape Town 1:250,000 scale*. Government Printer.
- Van Zyl, J. L. (1984). Interrelationship, among Soil Water Regime, Irrigation and Water Stress in the Grapevine (*Vitis vinifera* L.). (December): 276. Available at: <https://scholar.sun.ac.za>
- Vystavna, Y., Matiatos, I., & Wassenaar, L. I. (2020). 60-year trends of  $\delta^{18}\text{O}$  in global precipitation reveal large scale hydroclimatic variations. *Global and Planetary Change*, 195, 103335. <https://doi.org/10.1016/j.gloplacha.2020.103335>
- Watson, A., Eilers, A., & Miller, J. (2020). Recharge estimation using cmb and environmental isotopes in the verloreenvlei estuarine system, South Africa and implications for groundwater sustainability in a semi-arid agricultural region. *Water*, 12, 1362. <https://doi.org/10.3390/w12051362>
- Watson, A., Kralisch, S., Künne, A., Fink, M., & Miller, J. (2020). Impact of precipitation data density and duration on simulated flow dynamics and implications for ecohydrological modelling in semi-arid catchments in southern Africa. *Journal of Hydrology*, 590, 125280. <https://doi.org/10.1016/j.jhydrol.2020.125280>
- Watson, A., Kralisch, S., Miller, J., Vystavna, Y., Gokool, S., Künne, A., Helmschrot, J., Arciniega-esparza, S., Sanchez-murillo, R., & Birkel, C. (2024). Advancing isotope-enabled hydrological modelling for ungauged calibration of data-scarce humid tropical catchments. *Hydrological processes*, 38, 1–20. <https://doi.org/10.1002/hyp.15065>
- Watson, A., Künne, A., Birkel, C., Miller, J., Kralisch, S., Watson, A., Künne, A., Birkel, C., Miller, J., & Kralisch, S. (2024). Developing a model to assess the impact of farm dams and irrigation for data-scarce catchments. *Hydrological Sciences Journal*, 69(1), 1–18. <https://doi.org/10.1080/02626667.2024.2331790>
- Watson, A., Midgley, G., Künne, A., Kralisch, S., & Helmschrot, J. (2021). Determining hydrological variability using a multi-catchment model approach for the Western cape, South Africa. *Sustainability*, 13(24), 1–26. <https://doi.org/10.3390/su132414058>
- Watson, A., Miller, J., Fink, M., Kralisch, S., Fleischer, M., & De Clercq, W. (2019). Distributive rainfall-runoff modelling to understand runoff-to-baseflow proportioning and its impact on the determination of reserve requirements of the Verloreenvlei estuarine lake, west coast, South Africa. *Hydrology and Earth System Sciences*, 23(6), 2679–2697. <https://doi.org/10.5194/hess-23-2679-2019>
- Watson, A., Miller, J., Fleischer, M., & de Clercq, W. (2018). Estimation of groundwater recharge via percolation outputs from a rainfall/runoff model for the Verloreenvlei estuarine system, west coast, South Africa. *Journal of Hydrology*, 558, 238–254. <https://doi.org/10.1016/j.jhydrol.2018.01.028>
- Watson, A., Miller, J., Künne, A., & Kralisch, S. (2022). Using soil-moisture drought indices to evaluate key indicators of agricultural drought in semi-arid Mediterranean southern Africa. *Science of the Total Environment*, 812, 152464. <https://doi.org/10.1016/j.scitotenv.2021.152464>
- Watson, A., Vystavna, Y., van Rooyen, J., Miller, J., Kralisch, S., & Helmschrot, J. (2023). Towards the development of an isotope-enabled rainfall-runoff model : Improving the ability to capture hydrological and anthropogenic change. *Hydrological Processes*, 37, 1–17. <https://doi.org/10.1002/hyp.14819>
- Weaver, J. M. C., & Talma, A. S. (2005). Cumulative rainfall collectors—A tool for assessing groundwater recharge. *Water SA*, 31(3), 283–290. <https://doi.org/10.4314/wsa.v31i3.5216>
- Wohl, E., Barros, A., Brunzell, N., Chappell, N. A., Coe, M., Giambelluca, T., Goldsmith, S., Harmon, R., Hendrickx, J. M. H., Juvik, J., McDonnell, J., & Ogden, F. (2012). The hydrology of the humid tropics. *Nature Climate Change*, 2(9), 655–662. <https://doi.org/10.1038/nclimate1556>
- Wu, S., Tetzlaff, D., Yang, X., & Soulsby, C. (2022). Disentangling the influence of landscape characteristics, hydroclimatic variability and land management on surface water NO<sub>3</sub>-N dynamics: Spatially distributed modeling over 30 yr in a lowland mixed land use catchment. *Water Resources Research*, 58(2), e2021WR030566. <https://doi.org/10.1029/2021WR030566>

- Wu, Y., & Xu, Y. (2005). Snow impact on groundwater recharge in Table Mountain group aquifer systems with a case study of the Kommissiekraal River catchment South Africa. *Water SA*, 31(3), 275–282. <https://doi.org/10.4314/wsa.v31i3.5207>
- Yang, X., Tetzlaff, D., Müller, C., Knöller, K., Borchardt, D., & Soulsby, C. (2023). Upscaling tracer-aided ecohydrological modeling to larger catchments: Implications for process representation and heterogeneity in landscape organization. *Water Resources Research*, 59(3), e2022WR033033. <https://doi.org/10.1029/2022WR033033>
- Yoshimura, K., & Kanamitsu, M. (2008). Dynamical global downscaling of global reanalysis. *Monthly Weather Review*, 136(8), 2983–2998.
- Yoshimura, K., Kanamitsu, M., & Dettinger, M. (2010). Regional downscaling for stable water isotopes: A case study of an atmospheric river event. *Journal of Geophysical Research: Atmospheres*, 115(D18), D18114. <https://doi.org/10.1029/2010JD014032>

## SUPPORTING INFORMATION

Additional supporting information can be found online in the Supporting Information section at the end of this article.

**How to cite this article:** Watson, A., Birkel, C., Arciniega-Esparza, S., de Waal, J., Miller, J., Vystavna, Y., van Rooyen, J., Welham, A., Bong, H., Yoshimura, K., Helmschrot, J., Künne, A., & Kralisch, S. (2024). Evaluating input data sources for isotope-enabled rainfall-runoff models. *Hydrological Processes*, 38(9), e15276. <https://doi.org/10.1002/hyp.15276>